Norwegian University
of Life Sciences

**Master's Thesis 2024 30 ECTS**

Faculty of Medicine, Institute of Basic Medical Science at University of Oslo

# Exploiting tumour glycosylation for the personalised immunotherapy of breast cancer

Anny Nguyen

Chemistry and Biotechnology, Molecular biology

# Exploiting tumour glycosylation for the personalised immunotherapy of breast cancer

Anny Nguyen

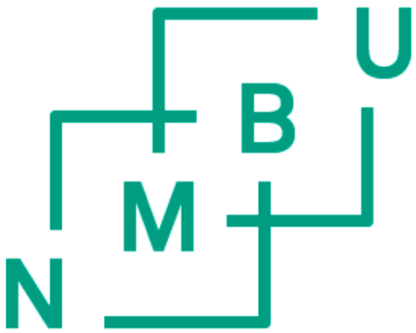


Supervisors

Michael Rory Daws

Erik Dissen

Harald Carlsen

Master's thesis

Faculty of Chemistry, Biotechnology and Food Science

Norwegian University of Life Sciences

May 2024

# Acknowledgments

This thesis project was performed during the spring of 2024, at the faculty of Chemistry, Biotechnology and Food Science at the Norwegian University of life Sciences in collaboration with the Faculty of Medicine at University of Oslo where the laboratory work was carried out.

I extend my deepest gratitude to my main supervisor, Professor Michael Rory Daws, whose expertise, understanding, and patience added considerably to my experience during this project. I appreciate your insightful guidance and encouragement, as well as invaluable feedback to push me in the right direction.

Further, a heartfelt thanks to PhD and senior engineer Elisabeth Gyllensten Bjørnsen and PhD student Ellen Sofie Pete, whom I have shared office with the past months, for taking me under their wings. I appreciate them for their warm welcome and good advice, you inspire me. I also owe a sincere appreciation to my co-supervisor Professor Erik Dissen for being critical (in the absolutely best way), challenge and engage me with insightful questions and discussion during our Tuesday meetings with the rest of NK-cell group and Receptors of the innate immune system group. A warm thanks to senior engineer Wendi Jensen for helping me in the laboratory, and to the whole immunobiology laboratory at UiO. I really appreciate the opportunity I got to be a part of the lab.

I also want to thank my supervisor Professor Harald Carlsen, at NMBU, for helping me with my many questions regarding the writing process.

I am deeply grateful for the opportunity to learn from and work with you all, your knowledge motivates me enormously.

# Abstract

Despite recent advances in undertanding the cancer genome, there is still a significant gap in understanding the complete characteristics of cancer's glycome and glycoproteome. Glycans play a crucial role in essential molecular and cellular processes that take place in cancer. These processes include cell signalling and communication, tumour angiogenesis, immune modulation and metastasis formation. Changes in glycosylation regulate the genesis and progression of the disease and also serve as significant biomarkers and offer specific targets for therapeutic intervention.

For this project, we wanted to look further into the expression of CLR ligands on cancerous cell lines and categorise them, as well as to generate CLR-CAR-NK cells and test their cytotoxic activity. Suitable CLR domains for tumour targeting and CAR construct would be chosen based on generated data, and thereafter, transfected into NK cells to test their cytotoxic activity against ligand-bearing cancer cells.

Tumour cells were screened for expression of CLR ligands. Ligand-binding domain of the CLR was fused with the human immunoglobulin Fc-domain, allows simple detection using secondary antibodies. The fusion proteins produced was used to directly stain tumour cells using flow cytometry. Tumour cells expressing a ligand will bind to the fusion protein allowing detection of ligand expression. Suitable CLR domains for tumour targeting and generate CAR construct were chosen based on the screening for expression.

The results from screening CLR ligand expression on cancerous cell lines were variable and differed from run to run. Nevertheless, the results did show some similarities or trends from run to run. Some problems occurred when ligation or and transfection of pUC19 and inserts were done. Therefore, few samples were sent for sequencing, which also ended up not matching the given sequences. As a result, it was not possible to move further on with the project due to the time limit.

In conclusion, even more FACS runs with fusion proteins for each cell line are necessary. This would provide a broader understanding of the CLR ligands expression. More trials (and errors) are also essential to eliminate potential sources of error when it comes to ligation and transfection of the CAR constructs. Ultimately, the results did not show that the CLRs were specific for each cell line and no CAR construct were successfully produced. However, with more time and testing on a larger scale, it could result in interesting findings.

# Sammendrag

Til tross for en stadig større forståelse av kreft genomet, er det fortsatt et betydelig gap i forståelsen av de fullstendige egenskapene til kreft glykomer og glykoproteom. Glykaner spiller en avgjørende rolle i essensielle molekylære og cellulære prosesser som finner sted i kreft. Disse prosessene inkluderer cellesignalering, kommunikasjon, tumor angiogenese, immunmodulering og metastase dannelse. Glykaner regulerer progresjonen av kreft gjennom endringer i glykosylering og fungerer også som betydelige biomarkører og tilbyr spesifikke mål for terapeutisk anvendelser.

For dette prosjektet var det ønskelig å se nærmere på uttrykket av CLR-ligander på kreftcellelinje og kartlegge dem. I tillegg til å produsere CLR-CAR-NK celler og teste deres cytotoksiske aktivitet. Der egnede CLR-domener for tumormålretting og CAR-konstruksjon vil bli valgt basert på genererte data. Deretter transfekter dem inn i NK-celler og test deres cytotoksiske aktivitet mot ligandbærende kreftceller.

Tumorceller ble screenet for uttrykk av CLR-ligander. Ligandbindende domene til CLR ble fusjonert med det humane immunglobulin Fc-domenet, noe som tillot enkel deteksjon ved bruk av sekundære antistoffer. Fusjonsproteinene som ble produsert ble brukt til å farge tumorceller direkte ved bruk av flow cytometri. Tumorceller som uttrykker en ligand, vil binde seg til fusjonsproteinet og tillater påvisning av ligandekspresjon. Passende CLR-domener for tumormålretting og genere CAR-konstruksjoner ble valgt basert på resultatene av screeningen av CLR ligander.

Resultatene fra screening av CLR-ligandekspresjon på kreftcellelinjer var variable og ulike fra kjøring til kjøring, med noen likheter eller trender fra kjøring til kjøring. Noen hindringer oppsto ved ligering og transfeksjon av pUC19 og inserts ble utført. Dette førte til at få prøver ble sendt til sekvensering, som også endte opp med å ikke ha samsvarende sekvenser. Det var derfor ikke mulig å gå videre med prosjektet på grunn av tidsbegrensning.

Til slutt, så er enda flere FACS-kjøringer med fusjonsproteiner for hver cellelinje nødvendig. Noe som ville gi en bredere forståelse av uttrykket av CLR-ligander. Flere forsøk (og feil) er også avgjørende for å eliminere mulige feilkilder når det gjelder ligering og transfeksjon av CAR-konstruksjonene. Resultatene viste ikke at CLR-ene var spesifikke for hver cellelinje, og ingen CAR-konstruksjon ble produsert med suksess. Med mer tid og testing i stor skala, kan resultere i interessante funn.

# Table of Contents

# List of figures

# List of tables

# Abbreviations

| | |
|---|---|
| **AIM2** | Absent in melanoma-2 |
| **ADCC** | Antibody-dependent cell-mediated cytotoxicity |
| **ALRs** | Absent in melanoma-2-like receptors |
| **Axi-cel** | Axicabtagene ciloceucel |
| **BSA** | Bovine Serum Albumin solution |
| **Bp** | Base pair |
| **CAR** | Chimeric antigen receptor |
| **CISH** | Cytokine checkpoint |
| **CLR** | C-type lectin receptor |
| **CRD** | Carbohydrate recognition domain |
| **CRS** | Cytokine release syndromes |
| **CTLA-4** | Cytotoxic T lymphocyte antigen 4 |
| **CTLD** | C-type lectin-like domain |
| **DAP** | DNAX – activation protein |
| **dNTP** | Deoxynucleoside triphosphates |
| **DMEM** | Dulbecco's modified eagle medium |
| **E-cadherin** | Epithelial cadherin |
| **ECM** | Extracellular matrix |
| **FACS** | Fluorescence-activated cell sorting |
| **FCS** | Foetal calf serum |
| **FSC** | Forward scatter |
| **GAGs** | Glycosaminoglycans |
| **GVHD** | Graft-versus-host disease |
| **HBP** | Hexosamine biosynthetic pathway |
| **HLA** | Human leukocyte antigen |
| **ICIs** | Immune checkpoint inhibitors |
| **IFN** | 1 Interferon |
| **IL** | Interleukin |
| **mAbs** | Monoclonal antibodies |
| **NK** | Natural killer |
| **NKG2** | Natural-killer group 2 |
| **NKG2C** | Natural-killer group 2 member C |

| | |
|---|---|
| **NLRs** | Nucleotide oligomerization domain like receptors |
| **NOD** | Nucleotide oligomerization domain |
| **PB** | PiggyBac |
| **PBS-EDTA** | Phosphate buffer saline – ethylenediaminetetraacetic acid |
| **PD-1** | Programmed cell death 1 |
| **PFA** | Paraformaldehyde |
| **PRR** | Pattern recognition receptors |
| **RIG-I** | Retinoic acid-inducible gene-I |
| **RLRs** | Retinoic acid-inducible gene-I-like receptors |
| **SB** | Sleeping beauty |
| **sLeA** | Sialyl Lewis a |
| **sLeX** | Sialyl Lewis x |
| **SSC** | Side scatter |
| **sTn** | Sialyl Tn |
| **TAAs** | Tumour-associated antigens |
| **Tisa-cel** | Tisagenlecleucel |
| **TLRs** | Toll-like receptors |
| **TNF** | Tumour necrosis factor |
| **TRAIL** | TNF-related apoptosis-inducing ligand |
| **UDP** | Uridine diphosphate |

# 1 Introduction

## 1.1 Immune system

The initial prompt reaction to a pathogen or altered cells is carried out by the innate immune cells (1). Immune cells consist of monocytes, neutrophils, macrophages, dendritic cells, natural killer (NK) cells, mast cells, eosinophils, and basophils (2). In contrast to T cells and B cells, which are highly specific, innate immune cells lack the expression of specific antigen recognition receptors (3). Pattern recognition receptors (PRRs) have a significant role in the immune system by recognising and binding to certain molecules found on the surface of pathogens, apoptotic host cells, and damaged senescent cells. This recognition induces effects, including anti-infection and anti-tumour effects, and also contributes to the initiation and execution of specific immune responses (3, 4).

With a variety of mechanisms, including the release of cytotoxic molecules, the engagement of more immune cells, the activation of the complement pathway, or the induction of the phagocytosis process, the cells of the innate immune system can control and clear invasion (5). In the context of cancer, tumour cells have the ability to release certain cellular components that could trigger the innate immune system. This would subsequently generate anti-tumour immunity within the microenvironment, ultimately leading to the eradication of the tumour (6, 7). Essentially, the growth of tumours can be regulated by the immune cells that are naturally capable of killing cancer cells. However, as the tumour progresses from abnormal tissue to tumours that can be detected clinically, cancer cells develop different mechanisms that mimic peripheral immune tolerance as the tumour progresses from neoplastic tissue to clinically detectable tumours (8).

Innate immune cell activation sets off a chain of actions that cooperate to control and destroy tumour cells. For instance, when transformed tumour cells are encountered, certain immune cells, such as dendritic cells and macrophages, become activated and release significant amounts of pro-inflammatory cytokines, such as type 1 interferon (IFN), interleukin (IL) 12 and IL-15, which stimulate the differentiation of T helper cells and NK cells (9, 10). Activation of innate cells releases large amounts of IFN-γ and chemokines, such as chemokine ligand 3 and chemokine ligand 4 a process that promotes the adaptive immune system (11-13). Together with an increase in major histocompatibility complex I (MHC I) molecules on tumour cells, the release of IFN-γ and IL-12 is also required to kill tumour cells by converting their anti-

inflammatory M2 to M1-phenotype (14, 15). Hence, determining the interaction between different cell types and tumour cells can therefore enhance our understanding of how immune cells infiltrate the tumour microenvironment, perhaps aiding in the selection of the most effective personalised immunotherapy therapeutic approaches (16).

### 1.1.1 Pattern recognition receptors

PRR are a category of receptors that have the ability to identify the particular molecular structure present on the surface of pathogens, apoptotic host cells, and damaged senescent cells. They can be categorised into five main families based on protein domain homology: Toll-like receptors (TLRs), nucleotide oligomerization domain (NOD)-like receptors (NLRs), retinoic acid-inducible gene-I (RIG-I)-like receptors (RLRs), C-type lectin receptors (CLR), and absent in melanoma-2 (AIM2)-like receptors (ALRs) (3).

As well as being present on the cell membrane, PRRs are also extensively distributed in the intracellular compartment membranes and the cytoplasm (17). Membrane-bound PRRs and PRRs in the cytoplasm are composed of ligand recognition domains, intermediate domains, and effector domains (18, 19). PRRs initiate downstream signalling pathways through the recognition of their ligands, which can result in various outcomes including the recruitment and release of cytokines, chemokines, hormones, and growth factors. The downstream signaling pathway can also induce chronic inflammation, forming an inflammatory microenvironment, initiating innate immune killing and subsequent acquired immune responses (4), maintaining the balance of the host microenvironment, and eliminating dead or mutated cells.

### 1.1.2 C-type lectin receptors

CLRs are a group of receptors that can recognise carbohydrates on the surface of pathogenic microorganisms with the engagment of $Ca^{+}$ (4). All CLRs with a carbohydrate recognition domain (CRD) can recognise carbohydrates. They are present on macrophages, dendritic cells, and certain tissue cells. Carbohydrate recognition domain mediates CLRs ability to recognise carbohydrates existing on self and non-self-structures (20). The carbohydrate recognition domain of CLRs has a compact spherical structure, and this region is referred to as C-type lectin-like domain (CTLD) (21, 22). CLRs are categorised as transmembrane receptors and secretory receptors depending on their position on the cell membrane (20, 23, 24).

Transmembrane receptors can be divided into type I and type II based on their topological structure and can either be type I or type II (25, 26). The N-terminal of type I receptors is oriented towards extracellular and can contain numerous carbohydrate recognition domains, whereas the N-terminal of type II receptors is oriented towards intracellular and can contain one carbohydrate recognition domain (27, 28), it is not given that all type I and II receptors have CRDs. CLRs are circular formations linked by two disulphide bonds, and contain at least one CTLD located outside the cell, while the intracellular domain varies (29).

The CLR CLEC 9A does not have a CRD and has been shown to bind to actin, which is an intracellular protein that is a part of the cytoskeleton. CLEC 9A recognise a conserved component when the cell membranes are damaged (30). Unlike other CLRs, CLEC 7A (also known as Dectin-1) does not have a typical CRD and is calcium independent, but it is still able to recognise carbohydrates (31). CLEC 4L (also known as DC-SIGN) functions both as a cell adhesion receptor and a PRR. As a cell adhesion receptor, it mediates the interaction between dendritic cells and T lymphocyte by binding to ICAM-3. They may also be present on normal cells as well as damaged cells (32). CLEC 8A (alternative name LOX-1) is a receptor for oxidized low-density lipoprotein (LDL) and is used for the absorption of LDL. LDL is a glycoprotein that transports lipids and cholesterol into the bloodstream. CLEC 8A has also been shown to bind to phosphatidylserine, which is on the cell surface of dying cells (33, 34).

## 1.2 Glycosylation

### 1.2.1 Glycosylation alteration in cancer

For more than six decades ago, changes in glycosylation linked to carcinogenic transformation were initially reported (35, 36). The accuracy of those observations was further supported by the introduction of monoclonal antibody technology. This demonstrated that tumour-specific antibodies targeted carbohydrates epitopes, which were primarily antigens found on tumour glycoproteins and glycosphingolipids (37, 38). When compared to their non-transformed counterparts, tumour cells exhibit a broad range of changes in glycosylation illustrated in figure 1.1. Protein glycosylation enhances the variability in molecular structure and the range of functions within groups of cells. The molecular heterogeneity is elevated due to abnormal glycan modifications, which are particular to each protein, occur at specific places (multiple sites on the same protein can have various glycosylation patterns), and are specific to certain cells. The intrinsic characteristics of the glycosylation process within a particular cell of tissue

type determine the specificities of glycosylation. Incomplete synthesis and neo-synthesis processes are the two main mechanisms that Hakomori and Kannagi initially proposed to explain the tumours-associated changes in carbohydrate structures (39). The result of impairment of normal synthesis of complex glycans found in healthy epithelial cells is due to an incomplete synthesis process, which also primary occurs in the early stages of cancer. This abnormality leads to the production of truncated structures, such as the expression of sialyl Tn (sTn) in gastrointestinal and breast cancer (40, 41). On the other hand, neo-synthesis, which is frequently detected in advanced stages of cancer, describes the cancer-associated induction of specific genes linked to the expression of carbohydrate determinants, as demonstrated by the de novo expression of certain antigens (such as sialyl Lewis A (sLeA) and sLeX) in many cancers (42).

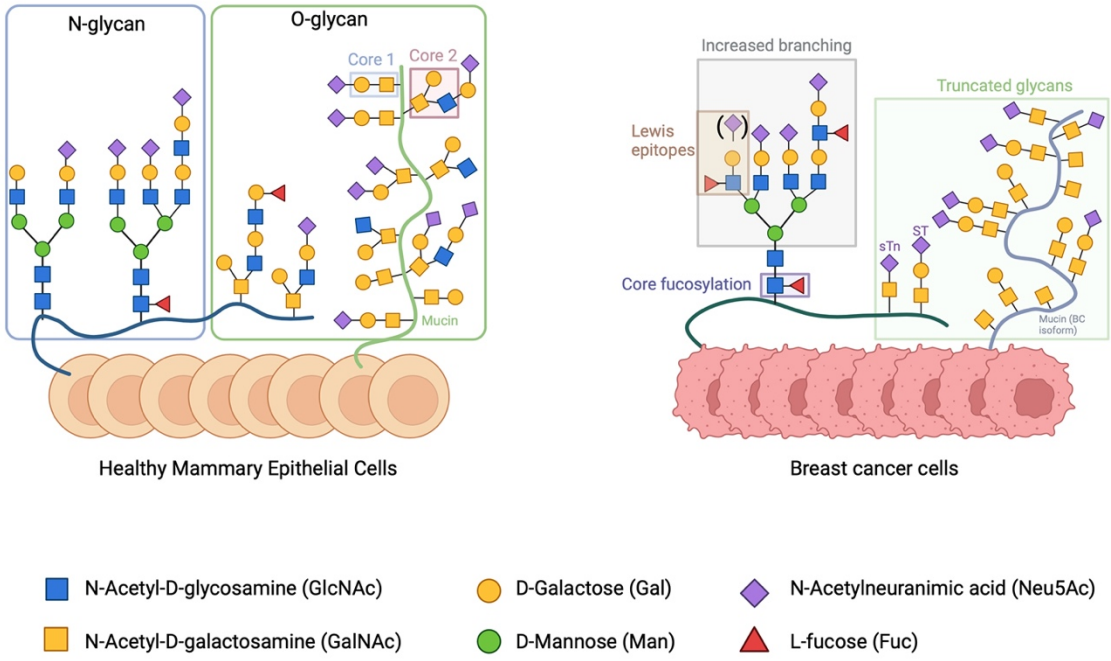


**Figure 1.1 Altered glycosylation patterns of glycoproteins on breast cancer cells.** Healthy mammary epithelial cells exhibit a variety of glycans on their surface. These glycans are connected by N-Acetylglucosamine GlcNAc to an aspargine site – N-glycans – or by a N-Acetylgalactosamine (GalNAc) to a serine/threonine site (mucin-type O-glycans). During the development of tumours, breast cancer cells undergo an abnormal production of glycans, which affects the way tumour cells interact with the surrounding microenvironment. The altered glycosylation in breast cancer involves elevated Lewis antigens (Lewisa and Lewisx: the sialyted Lewis X (sLeX) and Lewis A (sLeA)). Additionally, there is an increase in α1-6-core fucosylation and branching of N-glycans. Moreover, breast cancer typically exhibit a significant expression of truncated O-glycans, sometimes with terminal sialic acid (43-46). Created with BioRender.com, with inspiration from Lopes and Correia (47).

Cancer cells generally exhibit deviation from the normal glycosylation pathway, which results in altered expression of glycans due to one or more causes. First, irregularity of chaperone function (48, 49), and or altered glycosidase activity (50), as well as under- or overexpression of glycosyltransferases, can be the cause of altered expression of glycans. Second, changes in the tertiary conformation of the peptide backbone and that of the nascent glycan chain can also cause altered glycan expression. Third, the differences may result from the abundance and availability of sugar nucleotide donors and cofactors, as well as the diversity of variable acceptor substrates (51). Lastly, the localization of the glycosyltransferases in the Golgi apparatus may result in changes in the expression of glycan (52, 53).

Sialylation, fucosylation, O-glycan truncation and N- and O-linked glycan branching are the most widely occurring cancer associated changes in glycosylation (54-56). Since sialylation of carbohydrates is crucial for cellular recognition, cell adhesion, and signalling, sialylation is a significant change in cellular glycosylation. Reduction in the expression of glycosyltransferases has also been closely associated with cancer (57). Numerous fucosyltransferases (Fuc-Ts; Fuc-TI-Fuc-TXI) are responsible for the synthesis of fucosylated glycans. Fucosylation is a non-extendable modification that can be further subdivided into terminal fucosylation and core fucosylation (58). As often seen alteration in cancer cells during malignant transformation is the upregulation of complex β1,6-branched N-linked glycans (54, 59). The mannoside acetyl-glucosaminyltransferase 5 (MGAT5) gene encodes GnT-V, which is more active when GlcNAc-branching N-glycan expression is elevated. The overexpression of shortened O-glycans is another characteristic shared by tumours (60). The shortened or truncated glycans, such as the disaccharide Thomsen-Friedenreich antigen (T antigen, also known as core 1) and the mono-saccharide GalNAc (also known as Tn) and their sialylated forms (ST and STn (Neu5Acα2-6GalNAcα-O-R), respectively), which arise from the incomplete synthesis of O-glycans (61), ), are common forms of aberrant glycosylation that arise during malignancy.

### 1.2.2 Glycosylation in cancer cell

Several fundamental biological processes involved in cancer have been linked to glycans, including immune surveillance, cell-cell adhesion, inter- and intracellular signalling, cellular metabolism, cellular matrix interaction, and inflammation (60). Moreover, glycans alter the structure and conformation of proteins, which modulates their functional activity (62).

Deciphering the biological importance of glycan-based interactions in cancer can aid in the understanding of the molecular mechanisms underlying the biology of cancer (60).

#### *1.2.2.1 Tumour cell-cell adhesion*

A characteristic that contributes to the development of malignant tumours is the tumour cell's ability to evade cell-cell adhesion and infiltrate surrounding tissue. The transmembrane glycoprotein, epithelial cadherin (E-cadherin) (63), is a major epithelial cell-cell adhesion molecule in cancer (64). By directly interfering with E-cadherin-mediation, glycans can have a significant impact on tumour cell-cell adhesion. In cancer, there is a reciprocal regulatory mechanism between E-cadherin-mediated cell-cell adhesion and its glycosylation, which is regulated by the complementary actions of glycotransferases GnT-III and GnT-V, and can lead to either tumour metastasis or tumour suppression (65). Tumour associated antigens are highly expressed as a result of cancer cells' enhanced production of sialylated glycans (54, 66). Through the electrostatic repulsion of negative charges, the cell detaches from tumour mass. Which physically inhibits and disrupts cell-cell adhesion. This process is promoted by elevated expression of sialylated antigens (67, 68). Increased migration and decreased cell-cell adhesion are the outcomes of transfection of breast cancer cells with the sialyltransferase ST6Gal-I in vitro (69).

#### *1.2.2.2 Cell-matrix interaction and signalling*

The spatial context for the signalling events of different cell surface growth factor receptors is provided by the extracellular matrix (ECM), which consists of a diverse and intricate combination of glycoproteins, collagens, glycosaminoglycans (GAGs), and proteoglycans (70). Glycosylation has been demonstrated to significantly alter the activity and signalling of the multifunctional cell surface protein CD44 (71, 72), as well as to facilitate integrin dependent growth and survival (73, 74). Through the activation of c-Src signalling and the upregulation of stem cell proteins mediated by β-catenin, ceramide glycosylation in the cell membrane may have a proactive role in maintaining cancer stem cells (75). Additionally, proteoglycans are involved in the biogenesis and recognition of exosomes, which are endosomal-derived secretory vesicles involved in cell signalling (76).

#### *1.2.2.3 Cancer metabolism and signalling*

The Warburg effect, which refers to the shift from oxidative phosphorylation to aerobic glycolysis, characterised by high rates of glucose intake to meet the increased energetic and

biosynthetic needs to develop a tumour, is a crucial aspect of cancer cell metabolism (77). Cancer cells also upregulate glutamine absorption in an effort to fulfil the increased need for biosynthesis. Not only does the abundance of glucose in the cytoplasm of cancer cells contribute to increased glycolysis, but flux into the metabolic branch pathway also increases, such as the hexosamine biosynthetic pathway (HBP). Approximately 3-5 % of the total amount of glucose entering a cell is redirected through this pathway (78). Consequently, higher HBP flow is most likely caused by cancer cells absorbing more glucose and glutamine. Uridine diphosphate (UDP)-GlcNAc is the end-product of HBP and is a crucial metabolite that is needed for O-GlcNAcylation as well as O- and N-glycosylation (79). O-GlcNAc can function as a "nutritional sensor" due to its responsiveness to the glucose flux through O-GlcNAcylation (80). This increase in O-GlcNAcylation can lead to significant alterations in glycosylation by competing with other glycosylation pathways.

*1.2.2.4 Tumour immune surveillance*

Glycans interfere with tumour editing by regulating numerous aspects of the immune response. Various lectins, including galectins, C-type lectins, and siglecs, mediate this regulation by binding to glycans and controlling immunological processes, including those related to pathogen recognition, which in turn dictates the course of adaptive immune responses (81, 82). One important host defence mechanism known to prevent carcinogenesis and preserve cellular homeostasis is cancer immune surveillance. Immune effector cells have the ability to eradicate transformed cells, leading to the immunological selection of cancer cell types that are less immunogenic and resistant to immune effector cells. Through complement-dependent cytotoxicity, glycan-specific natural and induced antibodies (such as those against GM2, globo H, and $Le_y$) can mediate tumour cell killing and tissue destruction (83). Furthermore, aberrant O-glycosylation on the surface of cancer cells can trigger antibody-dependent cellular cytotoxicity (84). Aberrant O-glycosylation may interact with macrophage galactose-type C-type lectin (like MGL also known as CLEC 10A) (85) expressed on dendritic cells, and with dendritic cell-specific (like DC-SIGN also known as CLEC 4L) intercellular adhesion molecule-3 grabbing non-integrin 1 (86). CLEC 10A can be involved in helping tumours evade immune attack, by inhibiting macrophage attack, and instead makeing them develop an immunosuppressive phenotype (87).

## 1.4 Immunotherapy

Immunotherapy (including cytokine therapy, immune checkpoint inhibition, and chimeric antigen receptor (CAR)-T cell therapy) has expanded therapeutic options and improved the prognosis for patients with haematological tumours (88, 89). There was an advancement for the use of engineered T cells in haematological malignant tumours after four CD19 CAR-T cells, tisagenlecleucel (tisa-cel), axicabtagene ciloleucel (axi-cel), brexucabtagene autoleucel, and lisocabtagene maraleucel, products were approved (90-92). CAR-T cells have the ability to specifically target specific tumour antigens, hence augmenting the targeted toxicity of CAR-T cells has been utilised for the treatment of haematological malignancies (93). Although significant advancements have been made in the field of CAR-T cell-based immunotherapy for patients suffering from blood diseases, there are still limitations that impede its broader application in future treatment of haematological malignancies: (1) Cytokine release syndromes (CRS) and neurotoxicity are notable acute side effects that occur during CD19 CAR-T cell therapy (94); (2) on-target off-tumour effects may occur related to the recognition of molecular biomarkers that are also expressed on healthy tissues (e.g., B cell aplasia in anti-CD19/CD20 CAR-T cell therapy) (95); (3) antigen escape or loss may lead to disease relapse (e.g., typical CD19-negative relapse in B-cell malignancy) (96); (4) life-threatening graft-versus-host disease (GVHD) may be caused by allogeneic CAR-T cells (97).

NK cells are a part of the innate lymphoid cell family and are a type of cytotoxic immune cells that have been characterised their natural ability (98, 99). Humane NK cells exhibit a $CD3^-$ $CD56^+$ immunophenotype and may be divided into two subgroups: $CD56^{bright}CD16^{low-}$ cells, which represent a less mature population, and $CD56^{dim}CD16^{bright}$ cells, which represent a mature population of highly cytotoxic cells (100). NK cells primarily target tumours without the need for pre-sensitization or human leukocyte antigen (HLA)-matching, unlike T lymphocytes. Furthermore, clinical data indicates that the application of allogenic NK cells through adoptive transfusion hardly leads to GVHD (101-103). In addition, NK cells may provide protection against GVHD by specifically targeting the recipient's dendritic cells (104). Several techniques have been applied for NK cell-based immunotherapy. The addition of cytokines may enhance the activation, proliferation, and persistence of NK cells in both in vivo and in vitro (105). Numerous antibodies have been examined in order to enhance the killing activities of NK cells through several mechanisms: (1) monoclonal antibodies (mAbs), which target specific tumour-associated antigens (TAAs), have been approved for the treatment of

haematological malignancies based on NK cell-mediated antibody-dependent cell-mediated cytotoxicity (ADCC) (106); (2) CD16 BiKEs and CD16 TriKEs NK cell engagers are novel antibodies that can simultaneously bind two or three separate and unique antigens to strongly activate NK cell function, one is NK cell activating receptor CD 16 and the other one or two are TAAs (107); (3) mAbs that target immune checkpoints or their corresponding ligands could restore the anti-tumour function of NK cells (108, 109); (4) mAbs targeting NK cell inhibitory receptors (e.g., KIRs and NKG2A) also remain under investigation (110, 111). Lastly, transfusion of NK cells is an effective adoptive immunotherapy method to improve the number and the function of NK cells (112). These approaches to NK cell therapy can also be applied to CAR-NK cell therapy.

### 1.4.1 Checkpoint inhibition

In the field of personalised medicine and cancer therapeutics, there have been significant advancements in recent years (113). Immune checkpoint inhibitors (ICIs) are cancer immunotherapies that enhance anti-cancer immune response by specifically targeting inhibitory immunologic receptors on the surface of T-lymphocytes or their ligands (114). Consequently, in 2011, the approval of ipilimumab (115) marked the emergence of ICIs as a ground-breaking treatment option, revolutionizing cancer treatment (116). These medicines exhibited prolonged efficacy with reduced toxicity in certain situations (117). Unlike conventional therapeutic approaches, ICIs functions by stimulating the host immune system to fight cancer cells. Under homeostatic conditions, immune checkpoints maintain a balance of pro- and anti-inflammatory signals (118). These immunological checkpoints are a collection of inhibitory and stimulating pathways that regulate immune cell activity (119). On the surface of T cells, co-inhibitory receptors known as programmed cell death 1 (PD-1) and cytotoxic T lymphocyte antigen 4 (CTLA-4) are expressed to negatively regulate T cell-mediated immune response. Nevertheless, tumour cells take advantage of these inhibitory molecules to cause tumour tolerance and T cell exhaustion (120). Hence, ICIs including anti-CTLA-4, anti-PD-1 and anti-PD-L1 can bind to these co-inhibitory receptors, thus reinvigorating the immune response against tumour cells. Antibodies that specifically target these immune inhibitory receptors have been extensively utilised as immunotherapeutic treatments over the past ten years (121).

### 1.4.2 CAR-T cells to CAR-NK cells

A chimeric antigen receptor typically consists of four components: an extracellular binding domain, a hinge region, a transmembrane domain, and one or more intracellular signalling domains. The extracellular binding domain provides specificity to CAR-modified effector cells by targeting TAAs. The hinge region provides connection between the extracellular binding domain and the transmembrane domain (122). The composition of intracellular signalling domains, which play a crucial role in determining the strength of the activation signal and influencing the killing activity, varies in composition between the CAR generations. Initially, CARs were mostly composed of the CD3z activation signalling domain. However, in subsequent generations, CARs were enhanced by incorporating one or two supplementary costimulatory molecules, such as CD28, ICOS, 4-1BB, CD27, OX40 and CD40. CD28 and 4-1BB are the most utilised molecules among these (123, 124).

Chmielewski and his colleagues have developed the fourth generation of CARs, which provide effector immune cells with two transgenic products: the CAR itself and the transgenic payload. The primary focus on the fourth generation of CARs is to address the existing limitations of CAR-based cellular therapy, and thereby enhancing the capabilities of effector cells (125). DNAX – activating protein (DAP) 12, which is expressed in NK cells, takes part in signal of transduction that involves NK activation receptors natural-killer group 2 (NKG2) member C (NKG2C) and NKp44; DAP10 is also participating in signal transduction involving NKG2D (126, 127). Hence, DAP12 and DAP10 can transduce intracellular signals in CAR-NK cells. In addition, NK cells that were engineered with DAP12-based CARs exhibit superior performance compared to NK cells that were engineered with CD3z-based CARs (126).

### 1.4.3 Transduction of CAR-gene into NK cells

As of now, a significant obstacle arises due to the low transduction efficiency resulting from the absence of effective gene transferring approaches. The methods, viral transduction (retrovirus-based and lentivirus-based) and transfection (electroporation, lipofection, and in combination with transposon systems), used for the transduction of CARs into T cells can likewise be applied to NK cells (128). Viral transduction is illustrated in figure 1.2, these viral-based transduction approaches allow stable integration into the genomes of CAR-NK cells. The success of retroviral vector transduction in primary NK cells is greater with a 43-93 % higher efficacy. However, the insertional mutagenesis and deleterious impact associated with

this technique pose significant limitations in clinical applications (129). Even though lentivirus-based transduction is considered to be a safer method, the efficiency in peripheral blood mononuclear cells (PBMC) - derived NK cells are low (8-16 %) and still have to be improved (130). Even though RNA transfection methods are considered cost-effective approaches with higher gene transfer efficiency, it is important to note that production of CAR constructs with this method is temporary, typically lasting for roughly 3-5 days. While the limited therapeutic time window can be a disadvantage, the incidence of CAR-associated side effects, such as on-target off-tumour effects, may be decreased due to its transient nature (131-133). Utilisation of transfection methods with DNA integration techniques using transposon systems, such as PiggyBac (PB) and sleeping beauty (SB), has emerged as an appealing approach for production of transgene-expressing cells that are both safer and more stable (134, 135). The SB transposon vector has proven to be a highly effective and cost-effective approach for transferring genes. However, its suitability for use with CAR-NK cells has not been tested (136).

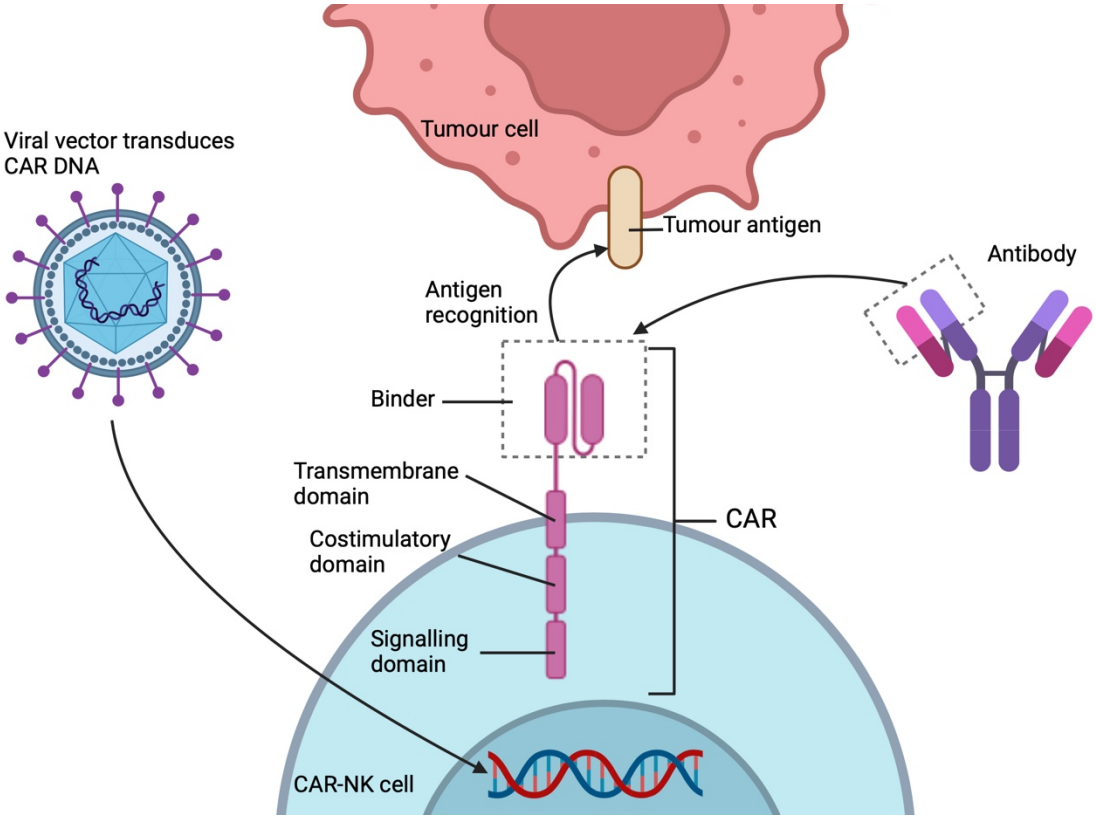


**Figure 1.2 Illustration of how a NK cell can be engineered to express CAR** using a monoclonal antibody's binder, which is represented by the single costimulatory domain. A viral vector is used to transfer the CAR DNA into the nucleus of the NK cell. Upon recognition of the tumour antigen, CAR initiates signal amplification and is transferred to the nucleus. Which results in a series of antitumour responses, where immune cells may proliferate and secrete cytokines, perforins, etc. Created with BioRender.com, with inspiration from Chan (137).

### 1.4.4 Advantages of CAR-NK compared to CAR-T cell therapy

CAR-NK cells are significantly safer compared to CAR-T cells. A frequently recognised adverse effect of CAR-T cell therapy are CRS and neurotoxicity. The abundance of cytokines released in the circulation, can result in symptoms such as high fever, sinus tachycardia, hypertension, hypoxia, depressed cardiac function and other organ dysfunction (94). The cytokine storm induced by CAR-T cells is mostly mediated by pro-inflammatory cytokines such as tumour necrosis factor-α (TNF-α), IL-1 and IL-6 (138). CAR-NK cells secrete a range of cytokines including INF-g and GM-CSF, which differ from the cytokines secreted by CAR-T cells. Furthermore, CAR-T cells from either autologous or allogeneic sources, have potential to induce life-threatening GVHD as a result of HLA restrictions. On the other hand, NK cells, which are considered important cells that mediate the early GVL response, can potentially prevent GVHD by eliminating recipient antigen-presenting cells (APCs) and cytotoxic T lymphocytes (139). Hence the utilisation of CAR-NK cells has the potential to address safety concerns associated with the clinical use of CAR-T cell products.

In addition, CAR-NK cells may have a superior effectiveness in targeting tumour cells compared to CAR-T cells. Initially, CAR-NK cells are capable of identifying and executing their killing effect through engineered killing capacity. By utilising CARs, effector cells are able to enhance their ability to superficially target and eliminate a particular antigen with greater efficiency. In comparison with CAR-T cells, CAR-NK cells retain the natural cytotoxicity of NK cells even when the expression of specific tumour antigens is reduced (140). NK cells recognise their target cells and subsequently perform biological function through multiple ways, including: (1) ADCC effect; (2) natural cytotoxicity; (3) TNF-related apoptosis-inducing ligand (TRAIL); and (4) FAS/FASL pathway (141). It is important to mention that NK cells maintain a dynamic equilibrium and complex interactions through several activating and inhibitory receptors. Upon activation, NK cells release cytotoxic granules containing effector molecules such as granzyme B and perforin, which effectively induce apoptosis in target cells. CAR-NK cells have additional costimulatory specificity, such as DAP10, DAP12 and 2B4, which provide more specific signalling in NK cells compared to CAR-T cells. These specialised molecules enhance the costimulatory specificity of CAR-NK cells beyond the shared CD28 and 4-1BB domains. Preclinical studies have shown that CAR-NK cells engineered with these costimulatory molecules, have an increased ability to destroy cancer cells (131, 142, 143).

Moreover, the production of CAR-NK cells is notably more convenient compared to the production of CAR-T cells. This is due to the absence of the risk of GVHD, NK cells can be obtained from either matched or HLA-mismatched donors. This allows for a wider range of potential donors and enhances the quality of the end products (144). Multiple sources of NK cells including NK92 cell lines, peripheral blood mononuclear cell-derived NK cells, umbilical cord blood-derived NK cells and induced pluripotent stem cell-derived NK cells, have been utilised for the production of CAR-NK cells. Therefore, the minimal likelihood of GVHD and the many origins of NK cells make them suitable as "off-the-shelf" goods that can be easily accessible for clinical applications (122).

### 1.4.5 Challenges and prospects of CAR-NK cells

Even though CAR-NK cells have many benefits in cancer immunotherapy, they nevertheless face hurdles that can impact their function and effectiveness, especially when compared to CAR-T cells. Unlike T cells and other human cells, NK cells have a greater susceptibility to the freezing and thawing process, resulting in diminished anti-tumour efficacy and lower survival rates. These restrictions may hinder the distribution of CAR-NK cells to distant places in an "on-demand" manner (145, 146). Moreover, the issue of restricted proliferation and persistence capacity poses a significant challenge in the application of NK cells and their engineered products for adoptive immunotherapy (145). Immunosuppressive cytokines such as TGFβ, adenosine, and indoleamine 2,3-dioxygenase are released in the tumour microenvironment and have detrimental effects on CAR-NK cells (147). Receptors that inhibit cellular activity, such as immune checkpoint molecules (TIGIT, PD-1, and CTLA-4, C-type lectin receptor (NKG2A), and cytokine checkpoint (CISH) , also play a role in the malfunctioning of CAR-NK cells (148). Hence, it is imperative to present future concerns and prospects in order to increase the efficacy of CAR-NK cell immunotherapy.

Improvement in CAR-NK cell constructions to address their limitations and maximise the capabilities of CAR-NK cells is crucial in the field of CAR-NK cell immunotherapy. Cytokines such as IL-2, IL-12, and IL-15 have a crucial role in boosting the effectiveness, persistence and expansion of NK cells in both innate and adaptive immunotherapy (149). Furthermore, the functionality of cryopreserved NK cells might be partially restored with additional IL-2 (150). Hence, utilising gene modification to transduce cytokine genes and knock off inhibitory genes in CAR-NK cells shows great potential. Due to the possibility of unforeseen toxicity caused by

excessive cytokine production from novel CAR-NK cells, including a suicide gene into CAR-NK cells is an important safety precaution. There has been shown that C9/CAR.19/IL-15 CB-NK cells can be easily eradicated by activating the iC9 suicide gene through pharmacologic activation in both preclinical and clinical studies (151, 152). In addition, it has also been shown that deletion of the CISH, a gene that encodes a cytokine checkpoint molecule, improves the metabolic fitness and antitumour effectiveness of armoured IL-15-secreting CD19 UBC-derived CAR-NK cells in lymphoma models (153). NK cells that have been engineered to express CARs and other foreign genes are referred to as "armoured" CAR-NK cells or "NK-cell pharmacies". These cells are capable of performing several activities (154). Furthermore, in order to avoid on-target off-tumour consequences in CAR-based immunotherapy relevant TAAs expressed solely on tumour cells must be identified and selected. Target antigens are frequently expressed on tumour blasts as well as healthy tissues in T-cell malignancies and myeloid tumours, which can be extremely toxic (155).

Recently, NKG2D ligands have been identified as promising novel targets, and the efficacy of NKG2D CAR-NK cells in treatment of MDS/AML and MM has been validated (156). Ongoing clinical trials are being conducted to gather comprehensive data on the novel engineered cells. Due to the distinctive natural cytotoxicity of NK cells, CAR-NK cells have the ability to selectively identify and eliminate tumour cells without relying on CAR signalling. Hence, developing a non-signalling CAR structure that prioritises homing-promoting target factors (such as chemokines and adhesion molecules) instead of target antigens that induce a direct killing signal, present a promising alternative. The novel CARs enable CAR-NK cells to accumulate tumour sites, allowing them to exert their function through NK cell-mediated mechanisms rather than relying solely on CAR-dependent mechanisms (128, 157). This may be more appropriate in lymphoma than in other haematological cancers due to the unique tumour site. Therefore, the "missing-self" mechanism of NK cells can potentially protect healthy tissue and cells against on-target off-tumour toxic effects (158).

To summarise, cytokines, immune checkpoint inhibitors, and monoclonal antibodies have the potential to augment the cytotoxicity of NK cells in adoptive immunotherapy. Moreover, the transfusion of CAR-NK cells with the approaches above could potentially augment the killing capacity and safety of CAR-NK cells.

# 2 Aims

Glycosylation, which is addition of sugar groups to proteins or lipids, is well established as a crucial alteration in tumour development. It has significant functions in cell signalling, cell-matrix interactions, angiogenesis, immune evasion, epithelial-mesenchymal transition and metastasis.

Over many million years, the immune system has developed to recognise abnormal changes in glycosylation. Sugar-binding C-type lectin receptors are a diverse set of pattern recognition receptors, which are mainly found on myeloid cells of the innate immune system (e.g. macrophages, granulocytes, dendritic cells). Over the course of several years, extensive research has been conducted on CLRs. CLRs from the two specific families Dectin-1 and Dectin-2, has been found to be involved in cancer.

This thesis will seek to exploit these receptors for the profiling and treatment of breast cancer. Given the important role of CLRs in regulating the activation of myeloid cells, it is probable that the tumour evade strategies will involve engagement of CLRs on myeloid cells in order to subvert the function of these cells. We will therefore screen tumours for the expression of CLR ligands. We have produced vectors for the optimised production of fusion proteins. These constructs fuse the ligand-binding domain of the CLR with the human immunoglobulin Fc-domain, which enables simple detection using secondary antibodies. The fusion protein will be utilised to directly stain tumour cells using flow cytometry, where tumour cells expressing a ligand will bind to the fusion protein allowing detection of ligand expression.

CAR-NK cells consist of a targeting domain (CLR ligand-binding domain in this case) coupled to a signalling domain that induces a cytotoxic response against ligand-bearing cells. Suitable CLR domains for tumour targeting and generating CAR construct will be chosen based on generated data. Afterwards, the CAR construct will then be transfected into NK cells tested for cytotoxic activity against ligand-bearing cancer cells.

To summarise the specific objectives:

I. Profile expression of CLR ligands on cancerous cell lines
II. Generate CLR-CAR-NK cells and test their cytotoxic activity

# 3 Materials and methods

## 3.1 Expression of CLR ligands on cell lines

All cell lines used in this thesis are listed in table 3.1, as well as their cell type, tissue, diseases they are derived from and if they are adherent or suspension cells (159-167). These cell lines were chosen due to the nature of the thesis aims, as well as the availability at the laboratory at the time. Jurkat-TAg and THP-1 were tested to conclude if they could be used as negative controls.

Each cell line has different changes in glycosylation, thereby if different CLRs can recognise the different changes in each cell line, it means that the CLRs are specific. Variation in glycosylation will result in variation in expression of CLR ligands on each cell lines. Differences in glycosylation among different cell line are determined by their compositions, cellular environment, and the specific set of glycosyltransferase they express (168).

**Table 3.1 Cell lines and their properties.** Overview of tumor cell lines used in this study: cell types, tissue, disease and if they are adherent and suspension cells.

| Cell line | Cell type | Tissue | Disease | Adherent/Suspension |
|---|---|---|---|---|
| **HET-1A** | Epithelial cell | Oesophagus | Normal | Adherent |
| **Jurkat-TAg** | T-cell | Peripheral blood | Lymphoblastic leukaemia | Suspension |
| **KYSE-450** | Squamous cell | Oesophagus | Carcinoma | Adherent |
| **MCF7** | Epithelial cell | Breast | Adenocarcinoma | Adherent |
| **MDA-MB-231** | Epithelial cell | Breast | Adenocarcinoma | Adherent |
| **SKBR3** | Epithelial cell | Breast | Adenocarcinoma | Adherent |
| **T-47D** | Epithelial cell | Breast | Carcinoma; ductal | Adherent |
| **THP-1** | Monocytes | Peripheral blood | Acute monocytic leukaemia | Suspension |
| **WM35** | Melanocytes | Skin | Cutaneous melanoma | Adherent |

### 3.1.1 Cell culture

To culture the cell lines, DMEM medium with antibiotic, foetal calf serum (FCS) and pyruvate was used. For sub-culturing the same medium was used, and the division ratio varied from cell line and was determined by how rapidly they grew and when they were going to be used the next time. The suspension cell lines were directly added to a 15 mL falcon tube. For adherent cells, medium was discarded and PBS-EDTA was added and incubated for 2-4 min to detach the cells from the wall of T75 flasks. Medium was added to the adherent cell lines and

transferred to 15 mL falcon tubes before the cells were centrifuged. The medium with PBS-EDTA was discarded and the cells were left as a pellet on the bottom of the tubes. The cells were then resuspended with medium before being transferred to new T75 (or bigger) flasks, and then diluted with more medium. The dilution ratio also depended on how well and fast the cells grew.

### 3.1.2 Fluorescence-activated cell sorting with fusion proteins

Fluorescence-activated cell sorting (FACS) is a specialised form of flow cytometry that allows for the separation of a heterogeneous population of cells tagged with fluorescence. This sorting process is done one cell at a time, based on the unique fluorescence properties of each individual cell (169). Anti-human IgG, Fcγ fragment specific secondary antibodies conjugated with phycoerythrin (PE) were used. The Fc-fusion proteins contain the Fc-region from human IgG1. The Fc-region has been mutated to prevent it from binding to the cell-surface Fc-receptors. This is crucial, otherwise it might bind to tumours that expressed Fc-receptors and would make it appear like the tumour had a ligand for the CLR even when if it did not. We are interested in the fusion proteins that bind to the tumour via the CLR domain, not via the Fc-region. FACS was utilised to detect the binding capacity of CLR ligands to each cell line, with help of secondary antibodies as fluorescens, illustrated in figure 3.1.

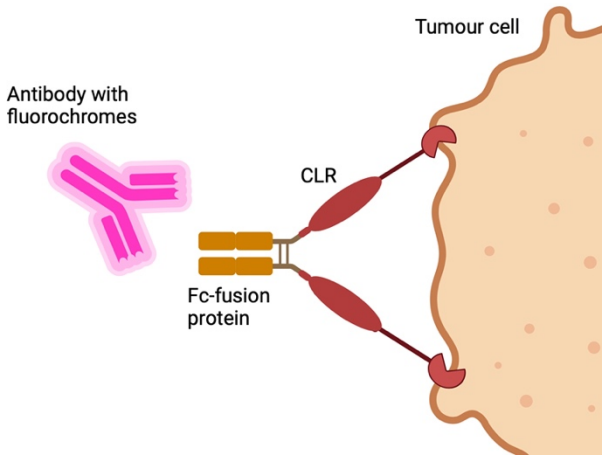


**Figure 3.1 How Fc-fusion protein, with CLR ligand, binds to tumour cells**. Illustration created with BioRender.com.

A test run with the cell lines SF126 and MDA-MB-231 were conducted to figure out how much fixing the cells affected the results, as well as figuring out the most optimal concentration of fusion proteins. From this test run, it was established that fixation had little to no impact on the results compared to cells that were not fixed. And that the optimal concentration of fusion proteins was between 4 – 8 µg/mL, therefore 8 µg/mL was used further on.

To run a FACS, 100 µL of approximately 2 – 2,5 million cells per mL was desired. The cells were split, then live cells were counted on an automated cell counter before diluting to the desired concentration. Subsequently the cells were transferred onto a V-shaped 96 well plate. The cells were then centrifuged at 1400 rpm, for 2 min at 4 °C, the medium was discarded by flipping the plate upside down before resuspending in 50 µL of PBS. When fixation was done on the test run, the cells were fixed with 50 µL of paraformaldehyde (PFA) into each well to obtain 2,0 % fixation before incubating on ice for 30 min (the cells were only incubated on ice if they were fixed). Afterwards a washing process was done 2 times: the cells were centrifuged (with the same settings on the centrifuge), the supernatant was discarded by flipping the plate upside down, 150 µL FACS was added and centrifuge again before the supernatant was discarded. Lastly, 120 µL of fusion proteins, listed in table 3.2, diluted to a concentration of 8 µg/mL were added before incubating in the fridge overnight.

**Table 3.2 Fc-fusion protein and their concentration.** Concentrations were used to calculate how many µL of each fusion protein that was needed to get 8 µg/µL per well.

| Fusion Protein Name | Concentration (µg/µL) |
|---|---|
| **CLEC 4D** | 1.82 |
| **CLEC 4E** | 0.94 |
| **CLEC 12A** | 1.08 |
| **CLEC 1B** | 1.1 |
| **CLEC 2D** | 1.84 |
| **CLEC 4L** | 1.05 |
| **CLEC 7A** | 1.4 |
| **CLEC 2A** | 2.72 |
| **CLEC 8A** | 1.38 |
| **CLEC 3B** | 1.2 |
| **CLEC 5A** | 2.5 |
| **CLEC 1A** | 0.66 |
| **CLEC 9A** | 2.04 |
| **CLEC 12B** | 0.18 |

The day after, the supernatant was discarded before the washing process was repeated 2 times. 100 µL of an antibody cocktail, with 25 µL antibody per 10 mL FACS, were transferred into each well, and then incubated at room temperature for 30 min in a dark space. The washing

process was then repeated 2 more times. Finally, the pellet was resuspended with 150 µL FACS buffer before it was run on the flow cytometer. The data was interpreted with FlowJo Software.

## 3.2 Generate CLR-CAR plasmid

3.2.1 Isolation of pUC19 and inserts

The pUC19 plasmid was digested with the enzymes Bam HI and Bgl II at 37 °C for 2 hours (or overnight) before pUC19 was cleaned with a QIAGEN PCR clean up kit following the manufacturer's protocol. This procedure removes primers, enzymes, salts and other impurities from the DNA sample, by using a microcentrifuge. Both this and QIAGEN gel clean up kit utilises columns and silica membrane assembly to bind DNA, in a high-salt buffer, before eluting the DNA with low-salt buffer. The silica-membrane eliminates the issues and inconvenience regarding resins and slurries.

**Table 3.3 Master mix for cutting pUC19**.

| Components | Volume (µL) |
|---|---|
| NEBuffer 3.1 (10 x) | 3 |
| Bam HI | 0,5 |
| Bgl II | 1 |
| Nuclease-free water | 20 |

The master mix in table 3.3 was made to cut pUC19 with restriction enzymes Bam HI and Bgl II and give the DNA sticky ends. To 5,5 µL of pUC19, 30 µL of the master mix containing NEBuffer 3.1 (10 x), Bam HI, Bgl II and nuclease-free water was added before digested on 37 °C for 2 hours. Afterwards 6 µL BpBlue dye (6 x) were added before a gel electrophoresis. A 1kB DNA ladder with BpBlue dye (6 x) on a 1 % low melting point agarose gel (with ethidium bromide) ran at 80 V, 400 mA for 2 hours.

After the gel electrophoresis, a picture was taken of the gels with a UV benchtop transilluminator, before cutting out the desired bands. pUC19 was isolated with a QIAGEN gel clean up kit following the manufacturer's protocol.

The vector, pUC19, was dephosphorylated afterwards to prevent the ends of the vector from sticking together. This was done by adding 10 µL Buffer Cut Smart, 2 µL calf intestinal

alkaline phosphatase (CIP) and 38 µL nuclease-free water to 50 µL of plasmid, then put on an incubator shaker at 37 ℃ for 30 min.

Before cutting the inserts, they were amplified with primers in table 3.4. Afterwards 6 µL BpBlue dye (6 x) were added to the samples before a gel electrophoresis, on a 1,5 % low melting agarose gel (with ethidium bromide). A 100 bp ladder with BpBlue dye (6 x) was used, and the samples ran for about 1 hour at 80 V and 400 mA. Subsequently, the samples were purified with a QIAGEN gel clean up kit following the manufacture's protocol.

**Table 3.4 Insert ligated into pUC19.** Primers used for each insert, as well as length of insert in base pair (bp).

| Referred name | Insert name | Length (bp) | Forward / Reverse primers |
|---|---|---|---|
| **DAP12** | hDAP12 | 135 | DAP12-GGBAM3 / DAP12-BGL5 |
| **DNAM** | DNAM1 | 171 | DNAM-GGBAM3 / DNAM-BGL5 |
| **CD3z** | CD3zeta | 345 | CD3Z-GGBAM3 / CD3Z-BGL5 |
| **4-1BB** | 4-1BB | 138 | 41BB-GGBAM3 / 41BB-BGL5 |
| **CD28** | CD28 | 126 | CD28-GGBAM3 / CD28-BGL5 |
| **CD30D** | CD30-distal | 189 | CD30D-GGBAM3 / CD30D-BGL5 |
| **CD30P** | CD30-proximal | 393 | CD30P-GGBAM3 / CD30P-BGL5 |
| **ICOS** | ICOS | 108 | ICOS-GGBAM3 / ICOS-BGL5 |
| **CD27** | CD27 | 147 | CD27-GGBAM3 / CD27-BGL5 |
| **2B4** | 2B4 | 189 | 2B4-GGBAM3 / 2B4-BGL5 |
| **OX40** | OX40 | 189 | OX40-GGBAM3 / OX40-BGL5 |
| **CRACC** | CRACC | 186 | CRACC-GGBAM3 / CRACC-BGL5 |

**Table 3.5 Master mix for cutting inserts**. The given volume is per sample

| Components | Volume (µL) |
|---|---|
| NEBuffer 3.1 (10 x) | 5 |
| Bam HI | 0,5 |
| Bgl II | 1 |
| Nuclease-free water | 3,5 |

After the inserts had been purified, 10 µL of the master mix in table 3.5 were added to each samples and digested at 37 ℃ for 1 hours. Then the samples were cleaned with a QIAGEN PCR clean up before stored in the freezer until further use.

Quantification of each insert and pUC19 was measured with Nanodrop. This was conducted in order to calculate the amount of each sample for further usage based on the measured concentrations.

### 3.2.2 Construction of new pUC19 vectors

#### *3.2.2.1 Ligation of pUC19 and inserts*

In order to construct the fragment for pUC19's new cloning site, the insert had to be cloned into pUC19. Both 1:4 and 1:1 ratio of purified product of pUC19 and each insert (from chapter 3.2.1 Isolation of pUC19 and inserts) were mixed together with nuclease-free water in PCR tubes, before running on the program "heat up", in figure 3.2, on the PCR instrument. This heats up the vectors and denature any end that are self-annealed, before cooling down in the presence of the insert so that the vector-ends and insert-ends anneals to each other instead. This will in theory make the ligation more efficient.

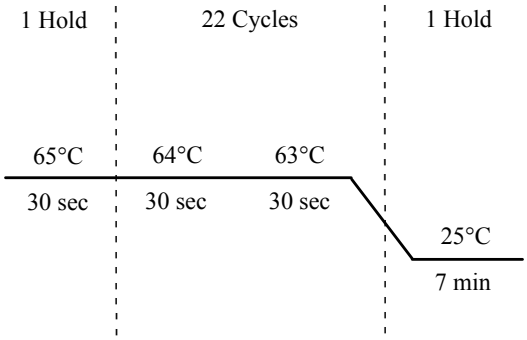


**Figure 3.2 PCR program "heat up"**. Cycles with temperature and durations.

After the "heat up" program had finished, 10 µL the ligation master mix in table 3.6 with ligase T4 DNA, 10 x Buffer for T4 DNA Ligase ATP and nuclease-free water was added to each tube before running a program named "ligation low temp" on the PCR instrument overnight. The program cycles are illustrated in figure 3.3.

**Table 3.6 Master mix for ligations** with components and volume given per sample, and therefore had to be multiplied with the total number of samples to make the master mix.

| Components | Volume (µL) |
|---|---|
| Ligase T4 DNA | 1 |
| 10 x Buffer for T4 DNA Ligase ATP | 2 |
| Nuclease-free water | 7 |

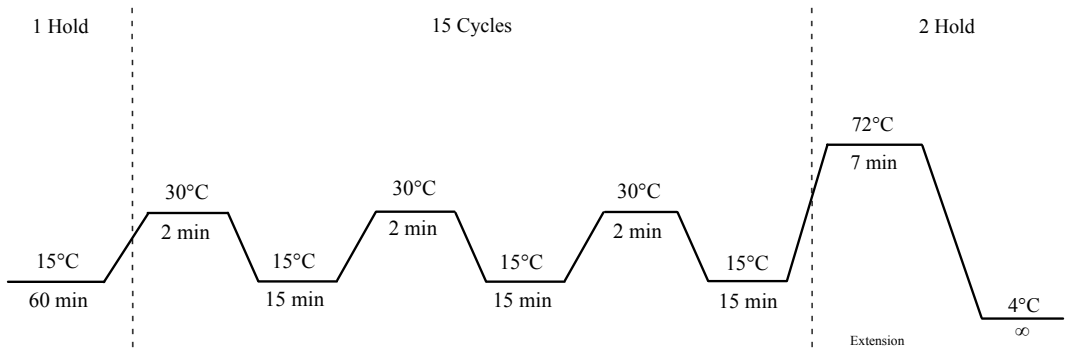


**Figure 3.3 PCR program "ligation low temp"**. Cycles with temperature and durations.

At 15 °C the enzymatic activity of most ligases, including T4 DNA ligase, is reduced compared to optimal conditions. However, the enzyme remains active enough to catalyse the ligation of the DNA fragments. Lower temperatures are beneficial for ligations involving sticky ends like these samples. The reduced kinetic energy at this temperature allows the sticky ends of DNA fragments to anneal more stably before the ligase enzyme seals them. This can result in higher specificity and potentially better yields for certain types of constructs. At 30 °C the enzymes are more efficient and speed up the reaction. The temperature boosts the kinetic energy of the DNA molecules and the ligase, facilitating faster collision rates between the ends, which can lead to a quicker sealing (170).

*3.2.2.2 Transfection of pUC19 and inserts*

After ligation, a transfection was conducted to introduce the plasmid into bacteria. This was done by adding the ligated product of pUC19 and each insert (from chapter 3.2.2.1 Ligation of pUC19 and inserts) to competent E. coli bacteria before incubating on ice for 30 min. Followed by 45 sec of heat shock at 42 °C, then incubated on ice for 2 min. 550 µL of SOC-bacteria medium was added to the samples before shaking in an incubator at 37 °C for 30 min. After the samples had been shaken for 30 min, 150 µL of each sample were plated out on agar plates (with ampicillin). The plates were incubated upside down with plastic film around at 37 °C overnight.

The day after transfection, colonies were picked. To a 96 well plate with 20 µL nuclease-free water in each well, colonies were picked with a pipette tip and placed in separate wells. 2 µL from each well was transferred to each PCR tube before adding 23 µL of the PCR master mix in table 3.7. Along with 1 µL of specific forward primer (in table 3.4) to each insert were added

to the PCR tubes. The PCR master mix contained reverse primer M13rev, dNTP, $MgCl_2$, 5 x GoTaq flexi buffer, GoTaq G2 flexi and nuclease-free water. Specific forward primers and the same reverse primer for each inserts, creates an extension to the inserts and makes the bands longer. Afterward the samples were run on the program "PCR-1" on the PCR instrument, following the cycles in figure 3.4. Lastly 150 µL of LB medium with ampicillin were added to each well before stored in the fridge until further use.

**Table 3.7 Master mix for PCR.** The volume given in this table is per sample and was multiplied with the total number of samples to make the master mix. The forward primers used for each sample was specific and not given in this table, but in a separate table 3.4.

| **Components** | **Volume (µL)** |
|---|---|
| M13rev | 1 |
| dNTP | 1 |
| $MgCl_2$ | 2 |
| 5 x GoTaq flexi buffer | 5 |
| GoTaq G2 flexi | 0,2 |
| Nuclease-free water | 12,8 |

The first initial hold at 94 ℃ is to cook the bacteria so that the DNA is released. At 94 ℃ the double-stranded DNA is denatured into single-strands. The high temperature breaks hydrogen bonds between the complementary bases of the DNA strands. Between 59-55 ℃ is the annealing stage where primers bind to the single-stranded DNA. This temperature depends on the melting temperature of the primers and is usually about 3-5 ℃ below the melting temperature. Extension of the DNA happens at 72 ℃, and synthesis of the new DNA strand from the dNTPs, using the single-stranded DNA as a template. DNA polymerase enzymes add nucleotides to the 3' end of each primer. After the last cycle, a final extension ensures that remaining single-stranded DNA is fully extended (171).

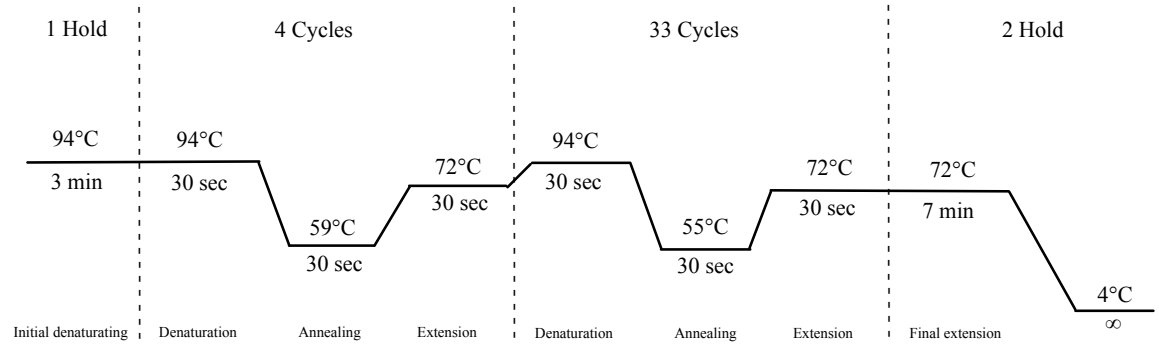


**Figure 3.4 PCR program "PCR-1".** Cycles with temperature, durations and the different phases.

After the program finished, the samples ran on a 1,5 % agarose gel containing ethidium bromide, along with a 100 bp ladder with BpBlue dye (6 x) at 80 V, 400 mA for 1 hour. No additional dye was added to the samples, because the 5 x GoTaq flexi buffer includes a green dye. For the samples that had the desired band at the right length: 50 µL of the solution in the 96 well plate and 3 mL of LBA medium were added to tubes and incubated in a shaker at 37 °C overnight.

After the samples had been shaken overnight, QIAprep spin miniprep kit following the manufacturer's protocol was conducted before the samples were sent for sequencing. The kit utilises columns and silica membrane that binds the plasmid in a high concentration of chaotropic salt before eluting the DNA in low-salt buffer. The results from sequencing were analysed on Benchling (172), where the sequences were compared to each other. Benchling was also used throughout the project for plasmid maps, visualising ligations in plasmid maps and for digital protocols.

### 3.2.3 CAR constructs

#### *3.2.3.1 Overlap extension PCR*

An overlap extension PCR is useful to create chimeric proteins without the use of restriction sites, which allows precise fusion. Designed overlap primers to contain at least 12 base pairs (bp) complementary to the end of the fusion partner DNA, which means that in the second phase we will have an overlap of at least 24 base pairs for annealing the two DNA fragments together. Which DNA fragments that were used, their primers and bp length, are in table 3.8.

**Table 3.8 Fusion product fragments** used for overlapping extension PCR with their primers and expected bp length after the overlap extension.

| Fragment # | Referred name | Length (bp) | Forward / Revers primers |
|---|---|---|---|
| 1 | **DCIR-TM** | 181 | SALSBF_hDCIR-F / DC4LOL-R |
| 2 | **CLEC 4L** | 991 | DCMIOL-F / ECOSTOP-CLEC4L-R |

The constructs utilises the DCIR-TM's transmembrane domain and CLEC 4L's extracellular domain. The DCIR-TMS's transmembrane domain allows a higher expression of the receptor. This may be a disadvantage, because the glutamine residues in the transmembrane of CLEC 4L may have some important structural role. 1 µL of each fragment (100 ng) and their primers were added to PCR tubes. Additional to 22 µL of a master mix for overlapping, seen in table 3.9, to each PCR tube. Subsequently, the samples were run on program "overlap extension 1" with the following cycle conditions in figure 3.5. Initial denaturation happens during the first phase at 94 ℃ for 30 sec, which prepares the double-stranded DNA for separation before the 33 cycles. In these 33 cycles, the denaturation phase happens at 94 ℃, followed by annealing at 55 ℃, and ending with extension at 72 ℃. The 33 cycles ends with a final extension phase to ensure that remaining single-stranded DNA is fully extended.

**Table 3.9 Master mix for overlap extension PCR** for the first run on "overlap extension 1" program. The volume given in this table is per sample and was multiplied with the total number of samples to make the master mix.

| Components | Volume (µL) |
|---|---|
| dNTP | 1 |
| $MgSO_4$ | 2 |
| NEBuffer 3.1 (10 x) | 2,5 |
| pfu | 0,5 |
| Nuclease-free water | 16 |

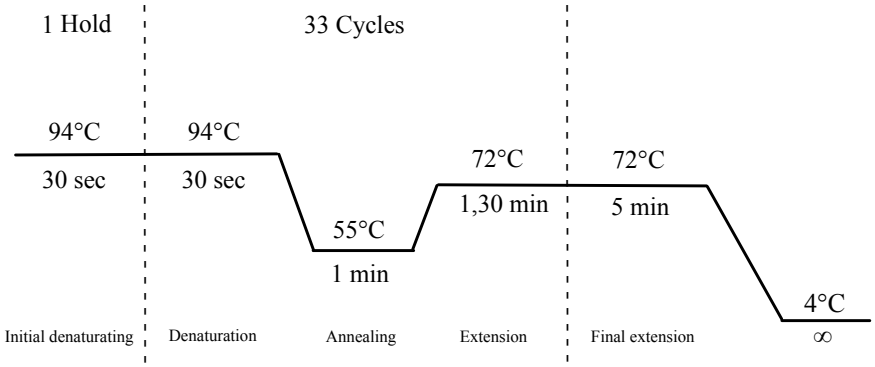


**Figure 3.5 PCR program "overlap extension 1".** The first run for overlap extension PCR with cycles, duration and the different phases.

After the cycles were finished, 5 µL of BpBlue dye (6 x) was added to each tube, before the fragments were purified on a 1,5 % low melting point agarose gel containing ethidium bromide alongside a 100 bp ladder with BpBlue dye (6 x), with the parameters: 80 V, 400 mA for 1 hour. An equimolar amount of the two fragments (approximately 10 nmol each) were prepared for the next PCR with the same master mix as in table 3.9, except without primers and more (2 µL) pfu. The program "overlap extension 2" ran overnight and following the cycle conditions in figure 3.6.

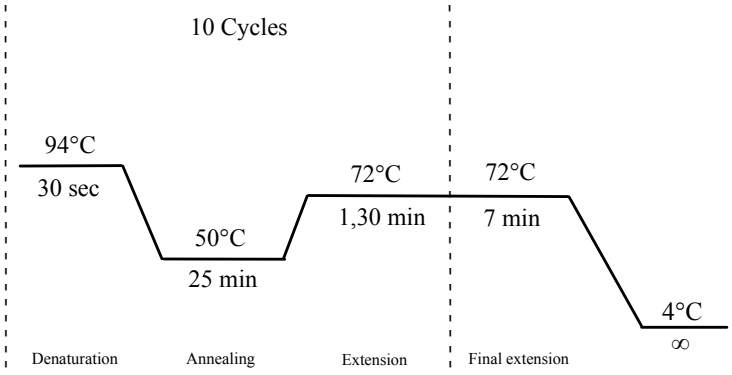


**Figure 3.6 PCR program "overlap extension 2".** The second run for overlap extension PCR with cycles, duration and the different phases.

The day after, 0,5 µL and 5 µL of the fusion product were amplified with primers in table 3.8 and by using the same master mix as in table 3.9, but the amount of Nuclease-free water was adjusted according to the concentration of the fusion product. Program "overlap extension 3" with cycle conditions in figure 3.7 below was used for amplifying.

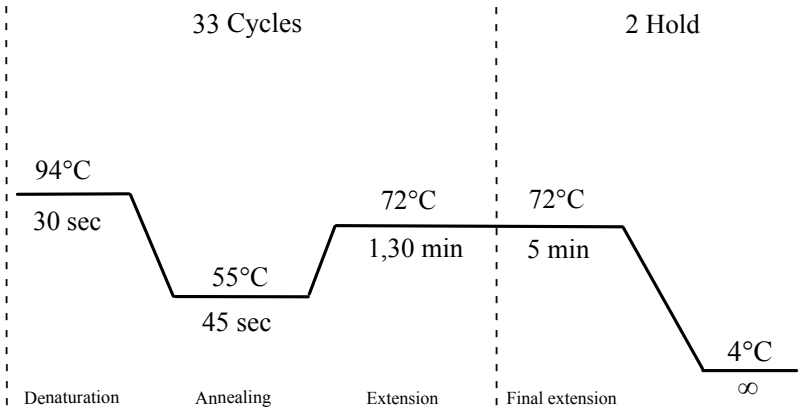


**Figure 3.7 PCR program "overlap extenstion 3".** The third and final run for overlap extension PCR with cycles, duration and the different phases.

After the last PCR run, the fusion product with 1 µL of both DCIR's forward primer and CLEC 4L's reverse primer, and 5 µL of NEBuffer 3.1 (10 x) was digested on 37 ℃ for 1 hour followed by 65 ℃ for 15 min. The samples were then cleaned with QIAGEN PCR clean up kit following the manufacturer's protocol before stored in the freezer until further use.

*3.2.3.2 Ligation of pScalps_puro and fusion product*

A plasmid with a lentiviral vector, pScalps_puro, was chosen, because of their ability to integrate their genetic material into the host cell's genome. This allows for a stable expression of the CAR gene, making them suitable to transduce highly replicating cells such as immune cells (173). Unlike other viral vectors, lentiviruses can infect both dividing and resting cells. This broad host range makes them more versatile for various therapeutic applications (174). Figure 3.8 illustrates how the finished construct of pScalps_puro with fusion product (DCIR-TM and CLEC 4) and a combination of inserts (A, B, C, D) are transduced into NK cells. The inserts itself and number of insert (A, B, C, D) will be chosen based on the data gathered from the FACS runs.

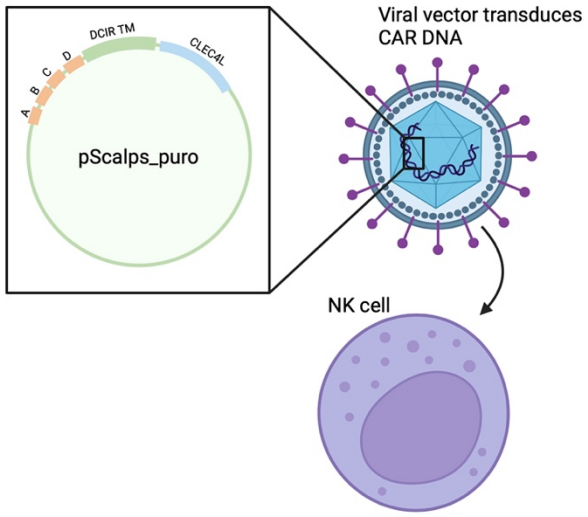


**Figure 3.8 Finished construction of pScalps_puro with fusion product and inserts.** Created with BioRender.com

The lentiviral vector pScalps_puro was digested at 37 ℃ for 2 hour followed by 65 ℃ for 15 min with the restriction enzymes XhoI (0,5 µL) and EcoRI (1 µL) and NEBuffer 3.1 (10 x) (5 µL). The samples were then purified on a 1,5 % low melting point agarose gel containing ethidium bromide with a 1 kB ladder with BpBlue dye (6 x), before a QIAGEN gel clean up kit was used following the manufacturer's protocol.

Ligation of the vector pScalps_puro with the fusion product, DCIR-TM and CLEC 4L, followed the same procedure as subchapter *3.2.2.1 Ligation of pUC19 and inserts*. Expect only a 1:4 ratio with vector and fusion product was used. The same PCR program was also used. The expected length of pScalps_puro with fusion product was expected to be 1141 bp. Thereafter a transfection was conducted following the same steps as subchapter *3.2.2.2 Transfection of pUC19 and inserts*.

### 3.3 Own contribution

Senior engineer Wendi Jensen produced the fusion proteins I used for my thesis, and my supervisor Professor Michael Rory Daws produced and isolated the competent E. coli bacteria for me. All primers were ordered from Eurofins. PhD and senior engineer Elisabeth Gyllensten Bjørnsen and PhD student Ellen Sofie Pete helped me with the setup for a big gel electrophoresis with 100 wells. This included making a TBE buffer and staining the gel with ethidium bromide afterwards. Elisabeth also kindly helped me make agar plates with ampicillin for transfection. For the FACSCalibur Flow Cytometer, Michael made the templates I used throughout the laboratory work.

The past four months of laboratory work, I have gained a solid overview of how I can plan my day, as well as work in a structured and efficient manner. Apart from those mentioned above, I performed all other experiments related to this thesis and analysed the gathered data from the FACS runs using FlowJo, excel and GraphPad.

# 4 Results

## 4.1 Expression of CLR ligands on cell lines

### 4.1.1 Test run

The first FACS run was conducted to determine the concentration of fusion protein for further experiments, as well as figuring out whether or not to fixative the cells. MDA-MB-231 with different concentration of fusion protein CLEC 4L are compared in table 4.1 and 4.2. ranging from control sample with 0 µg/mL to 32 µg/mL of fusion protein. Table 4.1 shows fixed cells, with 2 % PFA, and table 4.2 to the right show 0 % fixed cells. Firstly, by looking at fixed 2 % PFA compared to not fixed 0 % PFA, there are some differences, but not significant differences to the geometric means. This is further confirmed by comparing the same concentration of fusion protein with fixed cells versus cells that were not fixed, some small gaps, but no significant. Therefore, it was concluded to move further with 8 µg/mL of fusion protein and to not fix the cells.

**Table 4.1 Test run of MDA-MB-231 with fusion protein CLEC 4L and 2% PFA.**

| | Sample Name | Subset Name | Count | Geometric Mean : PE-A |
|---|---|---|---|---|
| | MDA MB231 CLEC4Lv1 2PFA_32.fcs | Live | 1864 | 1273 |
| | MDA MB231 CLEC4Lv1 2PFA_16.fcs | Live | 1783 | 793 |
| | MDA MB231 CLEC4Lv1 2PFA_8.fcs | Live | 601 | 1386 |
| | MDA MB231 CLEC4Lv1 2PFA_4.fcs | Live | 1384 | 1094 |
| | MDA MB231 CLEC4Lv1 2PFA_2.fcs | Live | 1809 | 728 |
| | MDA MB231 CLEC4Lv1 2PFA_1.fcs | Live | 1726 | 621 |
| | MDA MB231 CLEC4Lv1 2PFA_05.fcs | Live | 1798 | 613 |
| | MDA MB231 CLEC4Lv1 2PFA_0.fcs | Live | 1812 | 33,3 |

**Table 4.2 Test run of MDA-MB-231 with fusion protein CLEC 4L and 0% PFA.**

| | Sample Name | Subset Name | Count | Geometric Mean : PE-A |
|---|---|---|---|---|
| | MDA MB231 CLEC4Lv1 0PFA_32.fcs | Live | 1643 | 2083 |
| | MDA MB231 CLEC4Lv1 0PFA_16.fcs | Live | 1627 | 548 |
| | MDA MB231 CLEC4Lv1 0PFA_8.fcs | Live | 1478 | 1672 |
| | MDA MB231 CLEC4Lv1 0PFA_4.fcs | Live | 1588 | 1438 |
| | MDA MB231 CLEC4Lv1 0PFA_2.fcs | Live | 1585 | 911 |
| | MDA MB231 CLEC4Lv1 0PFA_1.fcs | Live | 1589 | 746 |
| | MDA MB231 CLEC4Lv1 0PFA_05.fcs | Live | 1598 | 1090 |
| | MDA MB231 CLEC4Lv1 0PFA_0.fcs | Live | 1590 | 48,4 |

### 4.1.2 Data from FACS runs

The results from the FACS runs were exported and analysed with the software FlowJo, which visualised the data into plots. Pseudocolour plots, the dotted plot below, display the relative population density of cell population within the gated area. The colour denotes areas of high and low population density. Here the Y-axis is side scatter (SSC), and X-axis is forward scatter (FSC). SSC measures scatter at a 90° angle relative to the laser, and FSC detects scatters along the path of the laser. FSC signals tells us about the cell size, and SCC tell us about the internal complexity of the cells (i.e. granularity). The histograms visualise the frequency distribution of the data versus fluorescence intensity, of the gated area from the pseudocolour plot.

The gate was adjusted for each control sample before the gates were transferred to the other samples of the same cell line for each individual FACS run. Afterwards, each cell line was compared to the different runs.

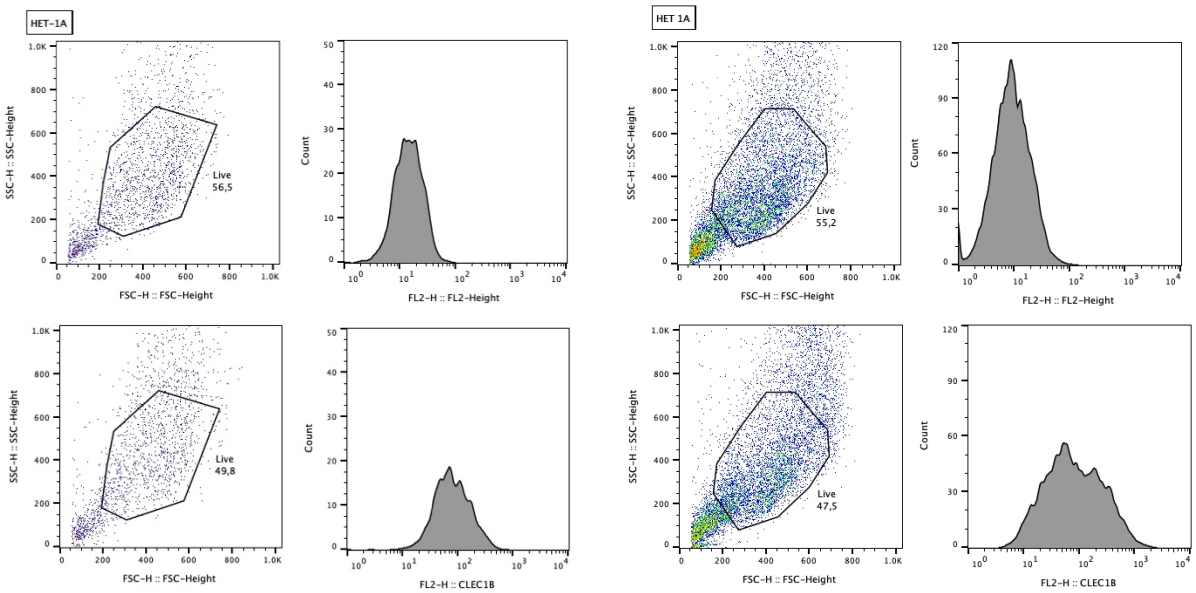


**Figure 4.1 Pseudocolour plots and histogram of HET-1A** from runs conducted the 02.02.24 to the left and the 21.03.24 to the right. The first row (of both runs on the left and right) are control without fusion proteins. Where the bottom row is with fusion protein CLEC 1B.

Pseudocolour plots and histograms in figure 4.1 are of the cell line HET-1A with fusion protein CLEC 1B and control (without fusion protein). The first row of plots are control samples, and the bottom row is with fusion protein, CLEC 1B. The histogram shows how much CLEC 1B are expressed on the HET-1A cells. The curve is further to the left on the X-axis on the histograms of the control samples, whereas the curve is further to the right on the X-axis with CLEC 1B. The further the curve is to the right of the X-axis, the more cells express the given fusion protein. The Y-axis of the histogram represent counted cells. It is worth mentioning that the Y-axis for the histograms for both runs have different scales, and that the run to the right counted significant more cells than the run to the left in figure 4.1

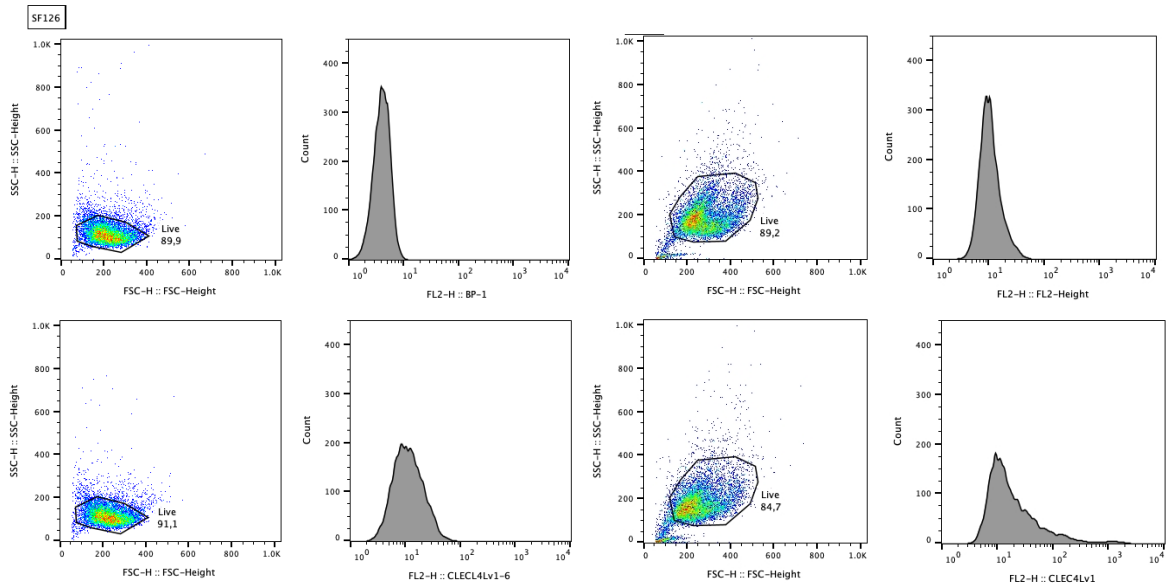


**Figure 4.2 Pseudocolour plots and histogram of SF126** from runs conducted the 13.02.24 to the left and the 21.03.24 to the right. The first row (of both runs on the left and right) are control without fusion proteins. Where the bottom row is with fusion protein CLEC 4L.

The size of SF126's cells are much smaller than the other cell lines screened. Therefore, two instrument settings and two acquisition settings were made for all the FACS runs. One for SF126, and one for bigger cells which were used for all the other cell lines. The first row of plots in figure 4.2 is of control samples without fusion protein, and the bottom row is SF126 with fusion protein CLEC 4L. Here the scale of the Y-axis is the same for both runs, which are the number of cells counted. These two runs of SF126 looks like to have counted approximately the same number of cells, unlike the two runs of HET-1A in figure 4.1.

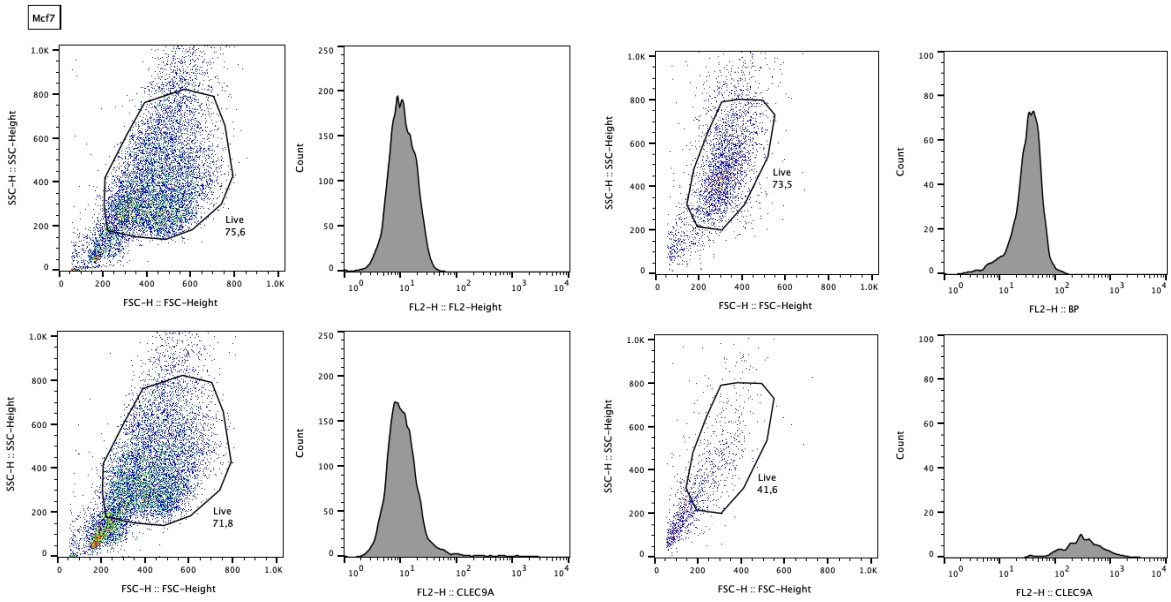


**Figure 4.3 Pseudocolour plots and histogram of MCF7** from runs conducted the 02.02.24 to the left and the 21.03.24 to the right The first row (of both runs on the left and right) are control without fusion proteins. Where the bottom row is with fusion protein CLEC 9A.

MCF7 without fusion protein (plots on the first row) and with fusion protein CLEC 9A (plots on the bottom row) are visualised in pseudocolour plots and histograms in figure 4.3, these plots are from runs conducted the 02.02.24 and the 21.03.24. Here, it is also worth mentioning that the Y-axis for the histograms for both runs have different scales. Much fewer cells were counted in the last run, compared to the first run, which do affect the comparison of these two runs.

To be able to compare the results more easily, the values of the control without fusion protein were used as normalizers. In this way the comparison of each FACS for each cell line was smoother. After the gates were adjusted in FlowJo, the data was exported into GraphPad to visualise the results in a bar chart for each cell line. Note that the geometric mean on Y-axis of each chart is in different scales, to make it more representable all the charts show 1 – 5 and from 5 and above it varies from cell line to cell line. Each colour represents different dates or batches of FACS runs, even though the cell lines are different.

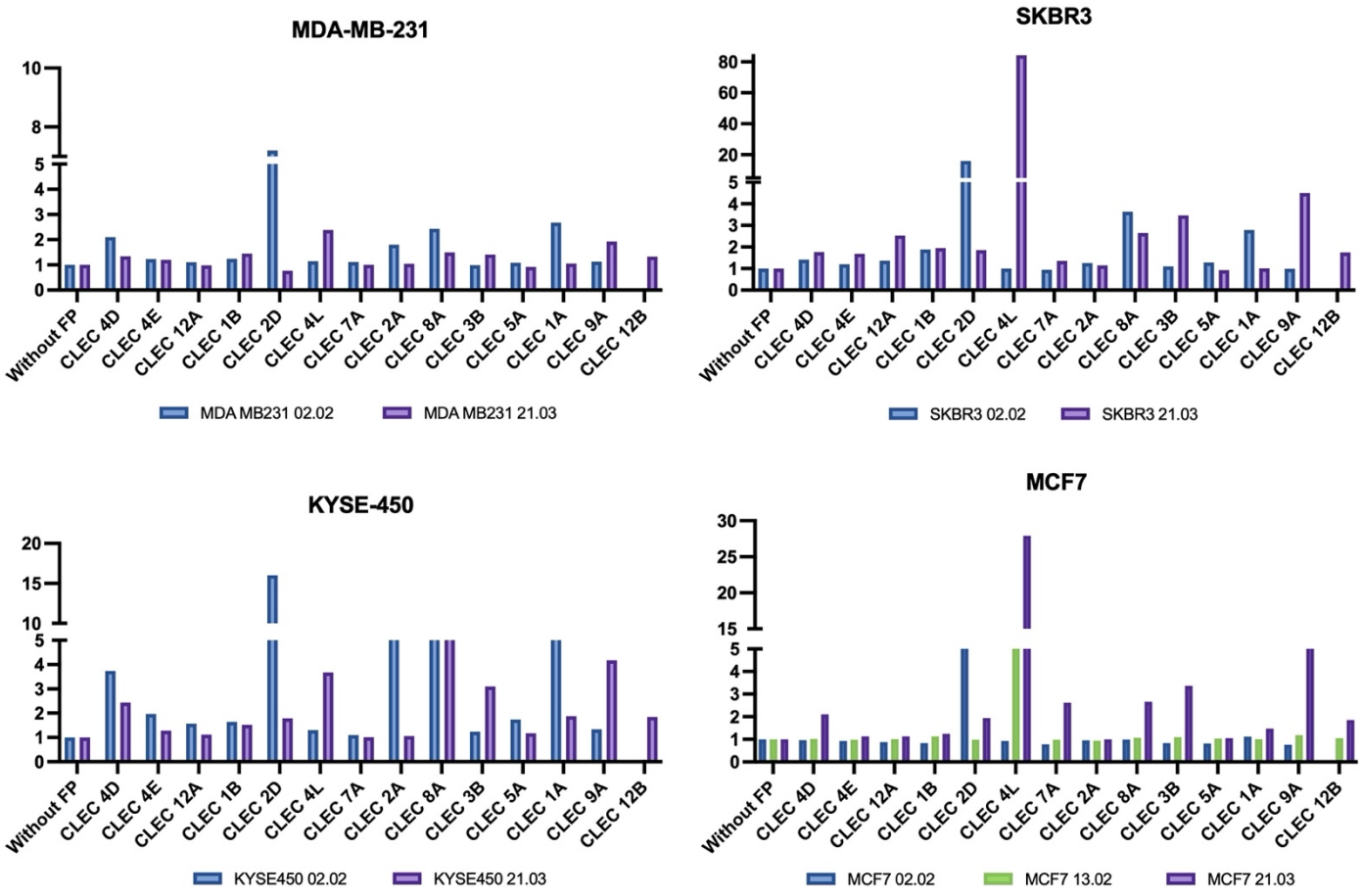


**Figure 4.4 FACS results of cell line MDA-MB-231, SKBR3, MCF7 and KYSE-450** with different fusion proteins, visualised as bar charts. Y-axis is geometric mean, where the control for each cell line for each run were used as a normalizer to make the comparison of the result easier. Note that the Y-axis scale for each cell line varies from 5 and above. The X-axis represents the different fusion proteins. The different colours of the bars represent dates of different FACS runs. Graphs created in GraphPad.

An overview of the FACS results for MDA-MB-231, SKBR3, MCF7 and KYSE-450 are visualised as bar charts in figure 4.4. Each colour in the charts represents dates of the different FACS runs. Indicating that regardless of the cell lines, the same colour of the bars implies that they were done on the same run. MDA-MB-231 has a higher expression of CLEC 2D compared to the other CLR ligands, in the first run (02.02.24) of this particular cell line. However, CLEC 2D is bound to multiple cell lines in this particular run conducted 02.02.24, it does not in other runs. KYSE-450 shows consistent expression for CLEC 8A in both of the FACS runs. CLEC 4D, CLEC 2A, CLEC 1A and CLEC 9A also show some expression in some of the runs. Several of the already mentioned CLR ligands that has shown expression, like CLEC 2D, CLEC 8A, CLEC 9A, are also expressed on SKRB3. In addition, CLEC 4L is strongly expressed on SKRB3 (on the last run). For MCF7, CLEC 4L are elevated on several runs, while CLEC 2D and CLEC 9A show greater expression in some of the runs.

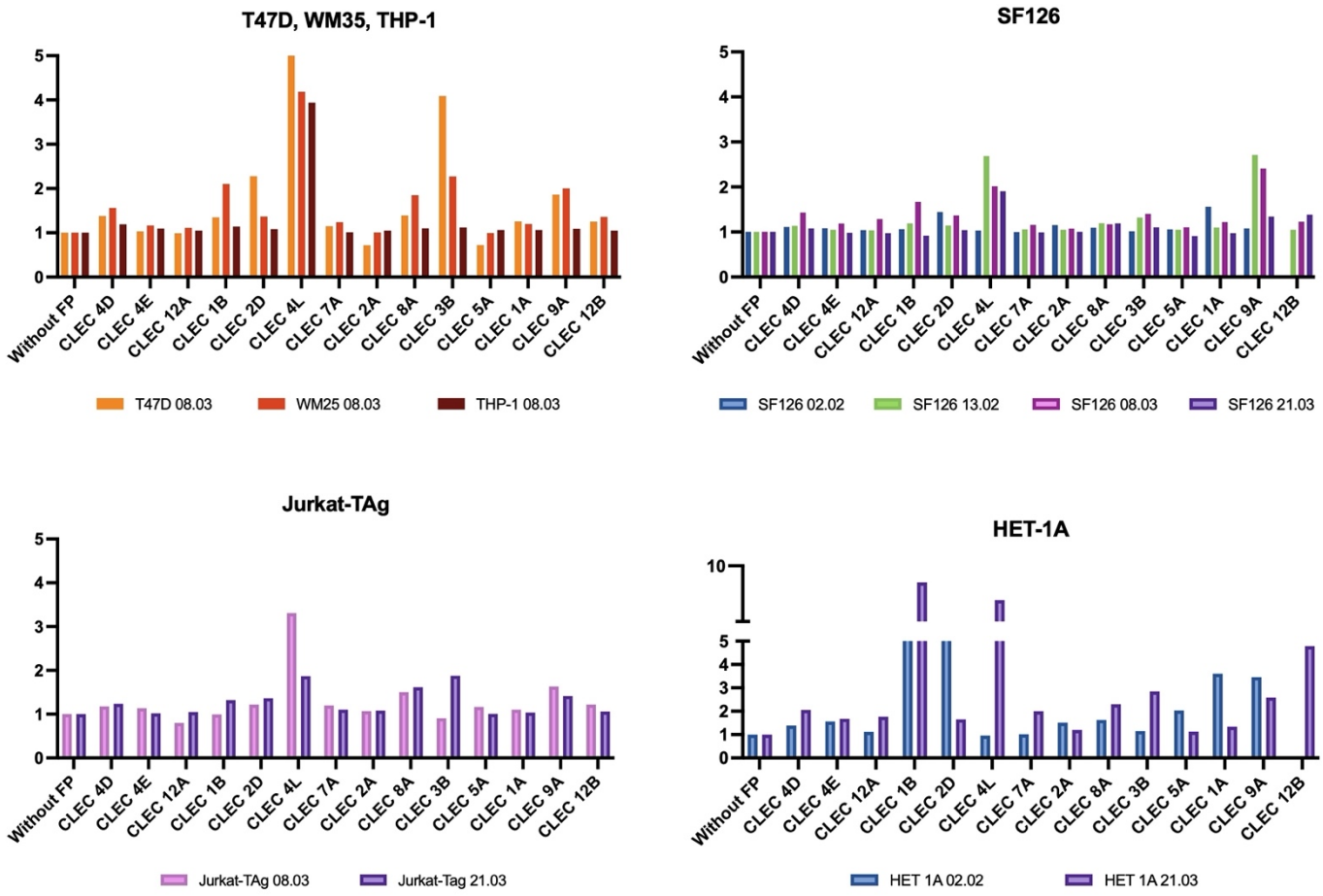


**Figure 4.5 FACS results of cell line HET-A1, SF126, Jurkat-TAg, T-47D, WM35, THP-1** with different fusion proteins, visualised as bar charts. Y-axis is geometric mean, where the control for each cell line for each run were used as a normalizer to make the comparison of the result easier. Note that the Y-axis scale for HET-1A is different from the other cell lines. The X-axis represents the different fusion proteins. The different colours of the bars represent dates of different FACS runs. The chart with T-47D, WM35 and THP-1 are from the same run, but were made in different shades of orange to represent the different cell lines. Graphs created in GraphPad.

SF126 was the cell line that grew fastest and was ready to be used whenever needed and is therefore also the one that was run most times. The expression of each CLR ligand is somewhat consistent overall. CLEC 4L and CLEC 9A have elevated expression compared to the other CLR ligands. WM35 has elevated expression of CLEC 4L, as does the cell lines T-47D, THP-1 and Jurkat-TAg. T-47D also shows expression of CLR ligand CLEC 3B. For HET-1A, there were different CLR ligands expressed, like CLEC 1B and CLEC 12B. It also showed that some of the already mentioned CLR ligands, CLEC 9A, 1A, CLEC 2D and CLEC 4L are expressed. Jurkat-TAg and THP-1 were tested to see if the cell lines were eligible as negative controls. As

negative controls, they had to show no expression to each fusion protein. They showed no or low expression of most CLR ligands, but CLEC 4L also bound well to these cell lines.

### 4.2 CAR constructs

After the ligation of pUC19 and inserts, a transfection followed by a gel electrophoresis was conducted to ensure the right bands. Figure 4.6 shows the results from the last transfections of pUC19 and several inserts, along with a 100 bp ladder. Name of each inserts are given under each band along with the number of the colony that was picked on the same agar plate.

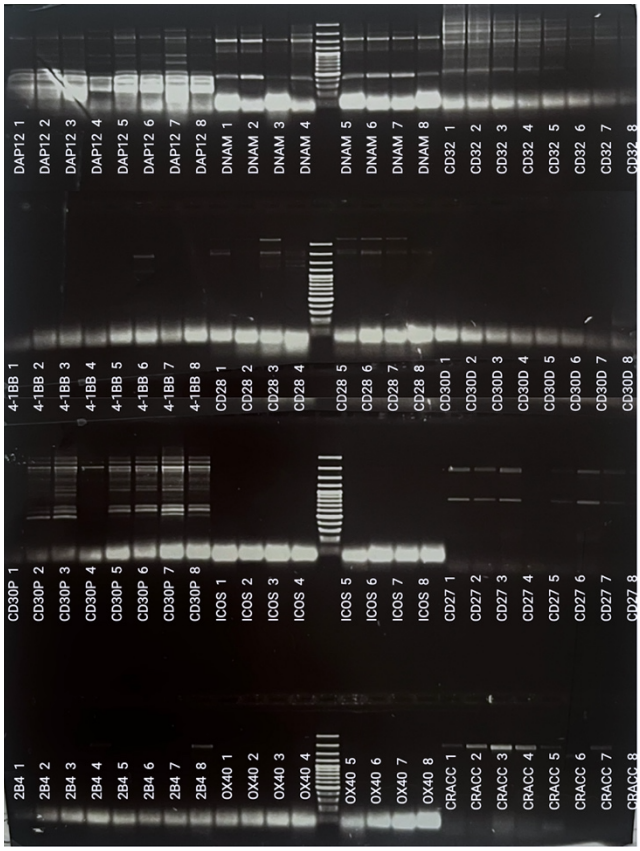


**Figure 4.6 Gel electrophoresis of pUC19 and inserts.** Inserts are given by name with the number of colony after each name.

Here there were several samples with multiple bands, as well as smeared bands. Some bands were also a lot bigger or smaller than expected. The bigger bands were too big to be a result of a self-ligated vector, or vector and two inserts. Some bands were even much smaller than the inserts themselves. Figure 4.7 explains the strategy for a correct ligation of insert. For a correct ligation, only on band is expected.

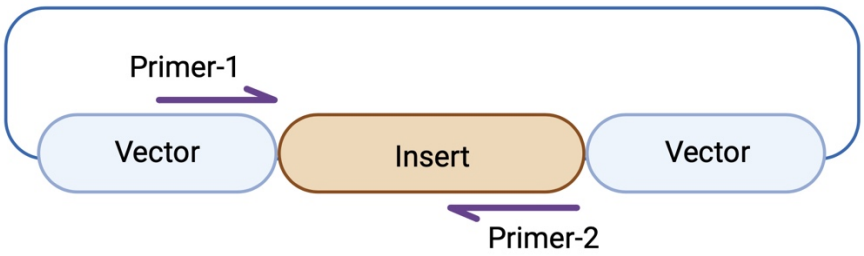


**Figure 4.7 Correct ligation of inserts and vector.** Illustration of desired ligation of insert and vector and the primers positions. Created with BioRender.com

Expected length of each insert along with primers used are in table 4.3

**Table 4.3 Inserts and expected length after ligation with pUC19.** Reverse primer M13rev createas an extension and makes the bands longer.

| Insert | Length (bp) | Forward / Reverse primers |
|---|---|---|
| **DAP12** | 206 | DAP12-GGBAM3 / M13rev |
| **DNAM** | 245 | DNAM-GGBAM3 M13rev |
| **CD3z** | 419 | CD3Z-GGBAM3 / M13rev |
| **4-1BB** | 209 | 41BB-GGBAM3 / M13rev |
| **CD28** | 197 | CD28-GGBAM3 / M13rev |
| **CD30D** | 254 | CD30D-GGBAM3 / M13rev |
| **CD30P** | 465 | CD30P-GGBAM3 / M13rev |
| **ICOS** | 182 | ICOS-GGBAM3 / M13rev |
| **CD27** | 218 | CD27-GGBAM3 / M13rev |
| **2B4** | 263 | 2B4-GGBAM3 / M13rev |
| **OX40** | 263 | OX40-GGBAM3 / M13rev |
| **CRACC** | 257 | CRACC-GGBAM3 / M13rev |

### 4.3 Sequencing

Several ligations with ratio 1:1 and 1:4 with pUC19 and insert, were conducted. As well as several transfection of the different ligation ratios. Few samples were sent to sequencing, because many gel electrophoresis did not have the right length on the bands. The few samples that were sent for sequencing were 6 samples of pUC19 with DAP12 and 4 samples of pUC19 with CRACC. The sequencing method was Sanger sequencing, and the results from the sequencing were exported to Benchling to compare the sequences. The sequencing did not match, therefore it was not possible to move further with any of the samples.

The next step for pScalps_puro with fusion product (DCIR_TM and CLEC 4), were to be sent for sequencing as well. Due to the time limit, the sample were not sent.

# 5 Discussion

To summarise; The results from this project were inconsistent. Firstly, the FACS results were variable and differed from run to run, even within the same cell line. On the other hand, some results could indicate a trend with similar results, but not identical or somehow predictable. This could be caused by several reasons. For the CAR constructs, even after several attempts and adjustment to the ligation and transfection, there were no successful results. Which also could be due to a couple of reasons.

Further, these are the key points that will be discussed:

I. Possible factors for inconsistent FACS results
II. Challenging aspects of CAR construction
III. Improvement potentials in the implementation

## 5.1 Expression of CLR ligands on cell lines

The test run conducted with MDA-MB-231 and fusion protein CLEC 4L (in table 4.1 and table 4.2) was to determine whether or not the cells needed to be fixed, and the optimal concentration of fusion protein. The geometric mean showed unsignificant differences between cells that were fixed with 2 % PFA and cells that were not fixed. And that the fusion protein concentration was optimal between 4-8 µg/mL of fusion protein. It was therefore decided to move further with an 8 µg/mL concentration of fusion protein, and to not fix the cells.

Overall, CLEC 4L binds consistently to several cell lines, except in the first run conducted 02.02.24. The same parameters and procedure were used this and the other runs. CLEC 4L may be presents on normal cells as well, which can make CLEC 4L-CAR-NK cells dangerous. NK cells “missing-self” mechanism can potentially protect healthy tissues and cells against on-target off-tumour toxic effect, which theoretically could eliminate the danger of CLEC 4L also being present on normal cells. By looking at figure 4.2 (in chapter 4.1 Data from FACS runs) and comparing the control of SF126, CLEC 4L are more expressed on the run conducted the 13.02.24, than the run conducted the 21.03.24. Which can be seen by looking at the curve on the histogram of the 13.02.24 is further to the right of the X-axis than the control from the same run. Additionally, this is visualised in figure 4.5 (in chapter 4.1.2 Data from FACS runs) with all the other runs of SF126 with CLEC 4L, where all runs with CLEC 4L have elevated expression.

CLEC 8A also gives consistent binding to some cell lines. CLEC 8A absorb LDL, which is a glycoprotein transporting lipids and cholesterol in the bloodstream. There may be that LDL is not bound to the cell surface here, and that CLEC 8A most likely are bound to something else here. Previous studies have shown that CLEC 8A binds to phosphatidylserine, which are present on the surface of dying cells. And although fewer MCF7 cells were counted on the run done the 21.03.24 a greater proportion of the cells expressed the CLEC 9A ligand compared to the first run done the 02.02.24. CLEC 9A is also one of the CLRs that does not have a CRD. Previous studies have shown that CLEC 9A binds to actin, which is an intracellular protein in the cytoskeleton. Actin is only available for binding if the cell membrane is damaged. Even though CLEC 9A does not have a CRD, it has not been established whether or not CLEC 9A is able to bind to sugar groups. Despite CLEC 7A does not have a CRD, it is still able to recognise sugar groups. This may suggest that CLEC 9A might recognise sugar groups despite missing a CRD. However, CLEC 2D are bound to many cell lines on the run conducted 02.02.24.

CLEC 1B binds consistently to HET-1A, but hardly at all to other cell lines. CLEC 3B binds nicely to T47D and WM35, but this is only one experiment. And CLEC 4D binds to KYSE-450 consistently. For MDA-MB-231 with CLEC 2D and SKBR3 with CLEC 4L and CLEC 2D, there is a wide gap of expression from each run. This also applies for other cell lines and other fusion proteins. These specific examples indicate that the different CLR ligands may not be specific, or at least not specific enough.

Although, there might be some debatable factors to this. Firstly, looking more closely at the results in retrospect, the number of cells were somewhat inconsistent. Especially looking at the two runs of MCF7. Even though the control (for each cell line) were used as a normalizer to make the results more comparable, the number of counted cells should be approximately the same. It was desirable to obtain between 2-2,5 million (live) cells per mL, cells were counted to calculate to get the right concentrations before conducting FACS runs. Some cells might not have survived overnight incubation since they were not fixed. Which again may have resulted in some dead cells, even though the initial concentration was obtained. This did affect the results, looking back at them. For this reason alone, more FACS runs should have been done.

Another possible cause for variation may be that cells change their glycosylation depending on where they are in the cell cycle. Therefore, it may be necessary to synchronize the cells in the cell cycle. Cells might also change their glycosylation depending on how dense the cells are. By growing the cells on a lower density in several large flasks, to be able to examine how they react in exponential growth phase and compare with completely confluent cells could also provide a greater understanding of how glycosylation and cell cycle affect each other.

Some other challenging aspects of this part of the project was to gather enough data, and at the same time conduct other experiments in the short time period of four months. Another difficulty was to time each FACS run. It was well known that the growth rate of each cell line was different, as well as the time the cell lines took to stabilise after defrosting. This led to multiple runs with fewer cell lines, which can be assumed was more time-consuming than fewer runs with many cell lines. More time to gather a representative amount of data, would give a better understanding of the CLR ligand expression trends or similarities.

## 5.2 Challenging aspects of CAR-construction

### 5.2.1 Ligation

Ligation of pUC19 and inserts were more challenging than expected. A possibility is that the ligations were successful, but that the PCR screen did not work properly. Since there were a lot of bands there, and there should only be one band if both vector and inserts are there. The temperature could have been raised to make the PCR more specific.

Some possible reasons for why the ligation did not work, could be because (1) the vector-insert ratio, (2) insufficient dephosphorylation of the vector or over reaction with CIP, (3) the purity and quality of both inserts and vector and (4) concentration of DNA. The vector and insert ratio were calculated based on the measured DNA concentration of both, as well as both 1:1 and 1:4 ratio was tested. Insufficient dephosphorylation may be a cause, which should prevent self-ligation and encourage insert incorporation. Over reaction with CIP can damage the ends, making them unable to ligate. Due to the length of some of the bands after previous electrophoresis, it could indicate that two vectors were ligated together instead of vector-insert ligation as desired. Even though the concentration was measured and calculated before every ligation, there may still be impurities after isolation of the DNA. Contamination like salts, ethanol or other residues from the DNA purification process can inhibit the ligation reaction.

Inhibition of the ligation process may also happen if other molecules in the reaction mix are present.

Other factors, that are more unlikely in this setting, which can play a role are incompatible overhangs, ligation efficiency of enzymes, temperature and duration of ligation. Incompatible overhangs are crucial due to restrictions enzyme's ability to cut the vector and insert to generate compatible overhangs. Restriction enzymes used were investigated beforehand to ensure that the vector and inserts were cut at the right sites. Even though, one of the restriction enzymes could have failed to cut properly or the restriction enzymes were cutting at the wrong place. This would be more unlikely if the conditions were correct. Temperature and duration of the programmed used were determined by several factors. T4 DNA ligase, which was used here, typically works best around 15 ℃ for sticky end ligation. Due to the low temperature, the reaction can be efficiently carried out overnight, and is more stable for annealing sticky ends without compromising the enzyme activity. Overnight ligation has also been shown to be more beneficial because it allows a more extended period for the DNA ends to successfully ligate to each other, increasing the overall yield of desired product.

### 5.2.2 Transformation

A transfection may face several hurdles that can lead to unsuccessful outcomes. Some factors might be (1) low transformation efficiency, (2) quality of competent cells, (3) quality of ligation product, (4) heat shock timing and temperature, (5) antibiotic selection, (6) presence of nucleases, (7) plasmid size and structure, (8) competent background growth or (9) plasmid compatibility and replication.

As discussed above, the quality of the ligation products and presence of nucleases in the samples from ligation are still valid factors for unsuccessful outcomes. Contamination of nucleases in the transformation mixtures can degrade the DNA of the plasmid, which reduces the effective concentration available for transformation. Contamination or the presence of other bacteria not targeted for transformation can outgrow and overshadow the transformed cells, especially if they are under stress from transformation. Larger plasmids or those with complex secondary structures can be more challenging to introduce into bacteria due to difficulties in the plasmid passing through the bacterial cell membrane.

The competent E. coli bacteria that were used for transfection, were also used by others (for other projects and purposes) with successful results, therefore low transformation efficiency and quality of competent bacteria are ruled out as a factor for the unsuccessful outcomes. The timing of heat shock and temperature might be a factor, but several precautions were made to avoid this. A stopwatch was always used to get the correct time, and the temperature was regulated with a thermometer (which was checked whether it worked or not before every heat shock was done). If the concentration of ampicillin was too high, it could inhibit the growth of successfully transformed cells. Conversely, if the antibiotic had degraded or the concentration was too low, it may allow the growth of non-transformed cells. This is also an unlikely factor, due to the same batch with agar plates with ampicillin and the same LB medium with ampicillin was used for every transfection conducted under this project. Which means the same batch with antibiotic both gave successful transfection with colonies and unsuccessful transfection with few colonies or colonies with (most likely) wrong ligation.

### 5.2.3 Electrophoresis

The length of the plasmids was determined by gel electrophoresis after ligation, where the bands were questionable. Since the size of some bands was approximately double the size of the vector itself, the initial thought was that dephosphorylation of the vector was insufficient, which could result in self-ligation. While other samples had several bands, which might be due to inadequate DNA purification or contamination of the samples. Some bands were also smeared or dragged. Possible reasons for smeared bands may be because of (1) degradation of DNA, (2) overloading of sample, (3) inadequate electrophoresis conditions, (4) poor quality or incorrect agarose, (5) incomplete restriction enzyme digestion or (6) issues with the buffer. DNA degradation can occur due to improper handling, storage or the presence of nucleases. In this context, incomplete restriction enzyme digestion can result in a mixture of cut and uncut DNA and can appear smeared on the gel.

Overloading of the samples is a less likely factor for the smeared bands, due to all the samples having the same amount loaded on the gel. And since not all the samples had smeared bands and only some of them, which also indicate that inadequate electrophoresis conditions, poor quality or incorrect agarose are unlikely factors. Inadequate conditions can be running the gel at too high voltage, which will lead to excessive heat generation and therefore might affect the migration of nucleic acids. Running the gel too slow can also lead to diffusion of bands. The

quality and concentration of agarose used to prepare the gel can impact the resolution of nucleic acids, where a low concentration of agarose is typically used for larger molecules and higher concentration of agarose is used for smaller molecules. Using the wrong concentration can lead to poor separation and smeared bands. Using an old or improperly made buffer can affect the pH and ionic strength, this might affect the migration of molecules through the gel and can result in smear or distorted bands.

Other adjustment, in addition to vector-insert ratio, that was tested to achieve the right ligation was several gel electrophoresis runs. Where different brands of low melting point agarose were tested, new isolation of vector pUC19 and regular Nanodrop measurements of each inserts and pUC19 to ensure DNA concentration. When isolating pUC19 again, time of digestion (from 2 hours to overnight) and time of dephosphorylation (from 30 min to 45-60 min) was extended to ensure sufficient digestion- and dephosphorylation results.

The majority of the ligated samples were not sent to sequencing, due to results after gel electrophoresis showed inconsistent length of bands. Of the 6 samples of pUC19 with insert DAP12 and 4 samples of pUC19 with insert CRACC, there were no sequences that matched. The method used, Sanger sequencing, is highly accurate for sequencing small to medium length of DNA and is often used for task that require high precision, like this and validating DNA sequences obtained by other methods. Therefore, it is presumable that the cause of incorrect sequences originates from earlier steps as discussed and not in the sequencing method itself.

# 6 Summary and conclusion

The aims of this project were to profile expression of CLR ligands on cancerous cell lines and generate CLR-CAR-NK cells, as well as test their cytotoxic activity. Unfortunately, due to unsuccessful ligations and or transfections it was not possible or time to move on to the next phase of the project. Which would be to finalise the CAR construct and introduce them into NK cells.

Regarding categorising expression of CLR ligands, there should have been conducted several more FACS runs to gather a representative amount of data to analyse. Despite the challenges concerning different growth rate of the cell lines and that there was preferable with fewer runs with multiple cell lines rather than multiple runs with fewer cell lines, in hindsight there would have been wiser to do multiple runs with fewer cell lines. Even though this would have been more time-consuming, more data could have been collected and the results would be more representable. Although more data would not necessarily have given a direct correlation of CLR ligand expression and cell lines or even similar trends, it would give a better understanding of whether this would be worth investigating further or not.

Furthermore, as for the unsuccessful ligations and or transfection for the CAR constructs, there might be some sources of error and some adjustment that could have been made. A possible source of error could be contamination during DNA isolation, purification and or impurities in the master mixes. And since all transfection used the same batch of agar plates, other agar plates could have been tested or that the specific batch with agar plates were contaminated or poorly made. It is hard to exactly pinpoint the reason for the unsuccessful outcomes here, but measurements to rule out where the fault may lie could have been taken to a greater extent. As well as trying other adjustments.

In conclusion, multiple FACS runs with fusion proteins for each cell line are required, preferable in multiple runs of each cell line. This would provide a broader understanding of the CLR ligands expression. More trials (and errors) are also necessary to eliminate potential sources of error when it comes to CAR constructs. Ultimately, the results did not show that the CLRs were specific for each cell line and no CAR construct were successfully produced. However, with more time and testing on a larger scale, it could result in interesting findings.

# 7 Future perspectives

To be able to use CLR ligands as biomarkers for the benefit of personalised immunotherapy, the expression of each ligand would have to be specific to each cell line or somehow be consistent to certain cell lines. Which as of now, unfortunately they don't seem to be. The conclusion is that it is necessary to explore CLR ligand expression on a bigger scale. Currently, there are not enough results to conclude with certainty whether or not they can be used as biomarkers for the benefit of personalised immunotherapy. In terms of the CAR construct, there are no obvious sources of error regarding the failed ligations and more trails are suggested.

If the results had been in our favour, the next phase of the experiment would have been to do a viral transduction of the lentiviral vector pScalps_puro, which includes a transmembrane domain (DCIR) and an extracellular domain (CLEC 4L), with a different selection of inserts. With the intention of creating a library collection of CLR-CARs with different inserts. And thereafter, transduce them into NK-cells.

Further, by utilising the CAR-NK cells for treatment of patient-derived xenograft-tumour bearing mice. Transferring xenografts to mammary fat pads of immunodeficient NSG mice and allow them to grow to a given size before commencing treatment with CAR-NK cells. Finally, injecting various numbers of CAR-NK cells intravenously or intratumorally and follow the subsequent growth of the tumours.

# References


1. Černý J, Stříž I. 2019. Adaptive innate immunity or innate adaptive immunity? Clin Sci (Lond) 133:1549-1565.
2. Kaur BP, Secord E. 2019. Innate Immunity. Pediatr Clin North Am 66:905-911.
3. Li D, Wu M. 2021. Pattern recognition receptors in health and diseases. Signal Transduction and Targeted Therapy 6:291.
4. Gajewski TF, Schreiber H, Fu Y-X. 2013. Innate and adaptive immune cells in the tumor microenvironment. Nature Immunology 14:1014-1022.
5. Iwasaki A, Medzhitov R. 2015. Control of adaptive immunity by the innate immune system. Nat Immunol 16:343-53.
6. Hagerling C, Casbon AJ, Werb Z. 2015. Balancing the innate immune system in tumor development. Trends Cell Biol 25:214-20.
7. Rolin J, Maghazachi AA. 2011. Effects of lysophospholipids on tumor microenvironment. Cancer Microenviron 4:393-403.
8. Gonzalez H, Hagerling C, Werb Z. 2018. Roles of the immune system in cancer: from tumor initiation to metastatic progression. Genes Dev 32:1267-1284.
9. Bellora F, Castriconi R, Dondero A, Reggiardo G, Moretta L, Mantovani A, Moretta A, Bottino C. 2010. The interaction of human natural killer cells with either unpolarized or polarized macrophages results in different functional outcomes. Proc Natl Acad Sci U S A 107:21659-64.
10. Helms MW, Prescher JA, Cao YA, Schaffert S, Contag CH. 2010. IL-12 enhances efficacy and shortens enrichment time in cytokine-induced killer cell immunotherapy. Cancer Immunol Immunother 59:1325-34.
11. Eisenring M, vom Berg J, Kristiansen G, Saller E, Becher B. 2010. IL-12 initiates tumor rejection via lymphoid tissue-inducer cells bearing the natural cytotoxicity receptor NKp46. Nat Immunol 11:1030-8.
12. Marcus A, Gowen BG, Thompson TW, Iannello A, Ardolino M, Deng W, Wang L, Shifrin N, Raulet DH. 2014. Recognition of tumors by the innate immune system and natural killer cells. Adv Immunol 122:91-128.
13. Corrales L, Matson V, Flood B, Spranger S, Gajewski TF. 2017. Innate immune signaling and regulation in cancer immunotherapy. Cell Res 27:96-108.
14. Berraondo P, Etxeberria I, Ponz-Sarvise M, Melero I. 2018. Revisiting Interleukin-12 as a Cancer Immunotherapy Agent. Clin Cancer Res 24:2716-2718.
15. Albini A, Brigati C, Ventura A, Lorusso G, Pinter M, Morini M, Mancino A, Sica A, Noonan DM. 2009. Angiostatin anti-angiogenesis requires IL-12: the innate immune system as a key target. J Transl Med 7:5.
16. Shihab I, Khalil BA, Elemam NM, Hachim IY, Hachim MY, Hamoudi RA, Maghazachi AA. 2020. Understanding the Role of Innate Immune Cells and Identifying Genes in Breast Cancer Microenvironment. Cancers (Basel) 12.
17. Mortaz E, Adcock IM, Tabarsi P, Darazam IA, Movassaghi M, Garssen J, Jamaati H, Velayati A. 2017. Pattern recognitions receptors in immunodeficiency disorders. Eur J Pharmacol 808:49-56.
18. Park BS, Lee JO. 2013. Recognition of lipopolysaccharide pattern by TLR4 complexes. Exp Mol Med 45:e66.
19. Yang X, Lin G, Han Z, Chai J. 2019. Structural Biology of NOD-Like Receptors. Adv Exp Med Biol 1172:119-141.
20. Dam TK, Brewer CF. 2010. Lectins as pattern recognition molecules: the effects of epitope density in innate immunity. Glycobiology 20:270-9.

21. Lepenies B, Lee J, Sonkaria S. 2013. Targeting C-type lectin receptors with multivalent carbohydrate ligands. Adv Drug Deliv Rev 65:1271-81.
22. Lan T, Li Z, Peng M, Niu D, Li Y, Li J. 2020. A four-CRD C-type lectin from razor clam Sinonovacula constricta mediates agglutination and phagocytosis. Gene 728:144287.
23. Sancho D, Reis e Sousa C. 2012. Signaling by myeloid C-type lectin receptors in immunity and homeostasis. Annu Rev Immunol 30:491-529.
24. Zelensky AN, Gready JE. 2003. Comparative analysis of structural properties of the C-type-lectin-like domain (CTLD). Proteins 52:466-77.
25. Hou H, Guo Y, Chang Q, Luo T, Wu X, Zhao X. 2017. C-type Lectin Receptor: Old Friend and New Player. Med Chem 13:536-543.
26. Mnich ME, van Dalen R, van Sorge NM. 2020. C-Type Lectin Receptors in Host Defense Against Bacterial Pathogens. Front Cell Infect Microbiol 10:309.
27. Brown GD, Willment JA, Whitehead L. 2018. C-type lectins in immunity and homeostasis. Nat Rev Immunol 18:374-389.
28. Li K, Underhill DM. 2020. C-Type Lectin Receptors in Phagocytosis. Curr Top Microbiol Immunol 429:1-18.
29. Robinson MJ, Sancho D, Slack EC, LeibundGut-Landmann S, Reis e Sousa C. 2006. Myeloid C-type lectins in innate immunity. Nat Immunol 7:1258-65.
30. Zhang JG, Czabotar PE, Policheni AN, Caminschi I, Wan SS, Kitsoulis S, Tullett KM, Robin AY, Brammananth R, van Delft MF, Lu J, O'Reilly LA, Josefsson EC, Kile BT, Chin WJ, Mintern JD, Olshina MA, Wong W, Baum J, Wright MD, Huang DC, Mohandas N, Coppel RL, Colman PM, Nicola NA, Shortman K, Lahoud MH. 2012. The dendritic cell receptor Clec9A binds damaged cells via exposed actin filaments. Immunity 36:646-57.
31. Huysamen C, Brown GD. 2009. The fungal pattern recognition receptor, Dectin-1, and the associated cluster of C-type lectin-like receptors. FEMS Microbiol Lett 290:121-8.
32. Geurtsen J, Driessen NN, Appelmelk BJ. 2010. Chapter 34 - Mannose–fucose recognition by DC-SIGN, p 673-695. *In* Holst O, Brennan PJ, Itzstein Mv, Moran AP (ed), Microbial Glycobiology doi:https://doi.org/10.1016/B978-0-12-374546-0.00034-1. Academic Press, San Diego.
33. Murphy JE, Tacon D, Tedbury PR, Hadden JM, Knowling S, Sawamura T, Peckham M, Phillips SE, Walker JH, Ponnambalam S. 2006. LOX-1 scavenger receptor mediates calcium-dependent recognition of phosphatidylserine and apoptotic cells. Biochem J 393:107-15.
34. Singh A, Srinivasan AK, Chakrapani LN, Kalaiselvi P. 2019. LOX-1, the Common Therapeutic Target in Hypercholesterolemia: A New Perspective of Antiatherosclerotic Action of Aegeline. Oxid Med Cell Longev 2019:8285730.
35. Ladenson RP, Schwartz SO, Ivy AC. 1949. Incidence of the blood groups and the secretor factor in patients with pernicious anemia and stomach carcinoma. Am J Med Sci 217:194-7.
36. Hakomori SI, Murakami WT. 1968. Glycolipids of hamster fibroblasts and derived malignant-transformed cell lines. Proc Natl Acad Sci U S A 59:254-61.
37. Feizi T. 1985. Carbohydrate antigens in human cancer. Cancer Surv 4:245-69.
38. Holmes EH, Ostrander GK, Clausen H, Graem N. 1987. Oncofetal expression of Lex carbohydrate antigens in human colonic adenocarcinomas. Regulation through type 2 core chain synthesis rather than fucosylation. J Biol Chem 262:11331-8.
39. Hakomori S, Kannagi R. 1983. Glycosphingolipids as tumor-associated and differentiation markers. J Natl Cancer Inst 71:231-51.

40. Julien S, Adriaenssens E, Ottenberg K, Furlan A, Courtand G, Vercoutter-Edouart AS, Hanisch FG, Delannoy P, Le Bourhis X. 2006. ST6GalNAc I expression in MDA-MB-231 breast cancer cells greatly modifies their O-glycosylation pattern and enhances their tumourigenicity. Glycobiology 16:54-64.
41. Marcos NT, Bennett EP, Gomes J, Magalhaes A, Gomes C, David L, Dar I, Jeanneau C, DeFrees S, Krustrup D, Vogel LK, Kure EH, Burchell J, Taylor-Papadimitriou J, Clausen H, Mandel U, Reis CA. 2011. ST6GalNAc-I controls expression of sialyl-Tn antigen in gastrointestinal tissues. Front Biosci (Elite Ed) 3:1443-55.
42. Kannagi R, Yin J, Miyazaki K, Izawa M. 2008. Current relevance of incomplete synthesis and neo-synthesis for cancer-associated alteration of carbohydrate determinants--Hakomori's concepts revisited. Biochim Biophys Acta 1780:525-31.
43. Cornelissen LAM, Van Vliet SJ. 2016. A Bitter Sweet Symphony: Immune Responses to Altered O-glycan Epitopes in Cancer. Biomolecules 6:26.
44. Cazet A, Julien S, Bobowski M, Burchell J, Delannoy P. 2010. Tumour-associated carbohydrate antigens in breast cancer. Breast Cancer Research 12:204.
45. Scott DA, Drake RR. 2019. Glycosylation and its implications in breast cancer. Expert Review of Proteomics 16:665-680.
46. Varki A, Cummings RD, Aebi M, Packer NH, Seeberger PH, Esko JD, Stanley P, Hart G, Darvill A, Kinoshita T, Prestegard JJ, Schnaar RL, Freeze HH, Marth JD, Bertozzi CR, Etzler ME, Frank M, Vliegenthart JF, Lütteke T, Perez S, Bolton E, Rudd P, Paulson J, Kanehisa M, Toukach P, Aoki-Kinoshita KF, Dell A, Narimatsu H, York W, Taniguchi N, Kornfeld S. 2015. Symbol Nomenclature for Graphical Representations of Glycans. Glycobiology 25:1323-1324.
47. Lopes N, Correia VG, Palma AS, Brito C. 2021. Cracking the Breast Cancer Glyco-Code through Glycan-Lectin Interactions: Targeting Immunosuppressive Macrophages. International Journal of Molecular Sciences 22:1972.
48. Schietinger A, Philip M, Yoshida BA, Azadi P, Liu H, Meredith SC, Schreiber H. 2006. A mutant chaperone converts a wild-type protein into a tumor-specific antigen. Science 314:304-8.
49. Aryal RP, Ju T, Cummings RD. 2010. The endoplasmic reticulum chaperone Cosmc directly promotes in vitro folding of T-synthase. J Biol Chem 285:2456-62.
50. Kakugawa Y, Wada T, Yamaguchi K, Yamanami H, Ouchi K, Sato I, Miyagi T. 2002. Up-regulation of plasma membrane-associated ganglioside sialidase (Neu3) in human colon cancer and its involvement in apoptosis suppression. Proc Natl Acad Sci U S A 99:10718-23.
51. Kumamoto K, Goto Y, Sekikawa K, Takenoshita S, Ishida N, Kawakita M, Kannagi R. 2001. Increased Expression of UDP-Galactose Transporter Messenger RNA in Human Colon Cancer Tissues and Its Implication in Synthesis of Thomsen-Friedenreich Antigen and Sialyl Lewis A/X Determinants1. Cancer Research 61:4620-4627.
52. Kellokumpu S, Sormunen R, Kellokumpu I. 2002. Abnormal glycosylation and altered Golgi structure in colorectal cancer: dependence on intra-Golgi pH. FEBS Lett 516:217-24.
53. Gill DJ, Chia J, Senewiratne J, Bard F. 2010. Regulation of O-glycosylation through Golgi-to-ER relocation of initiation enzymes. J Cell Biol 189:843-58.
54. Hakomori S. 2002. Glycosylation defining cancer malignancy: new wine in an old bottle. Proc Natl Acad Sci U S A 99:10231-3.
55. Christiansen MN, Chik J, Lee L, Anugraham M, Abrahams JL, Packer NH. 2014. Cell surface protein glycosylation in cancer. Proteomics 14:525-46.

56. Arnold JN, Saldova R, Hamid UM, Rudd PM. 2008. Evaluation of the serum N-linked glycome for the diagnosis of cancer and chronic inflammation. Proteomics 8:3284-93.
57. Kim YJ, Varki A. 1997. Perspectives on the significance of altered glycosylation of glycoproteins in cancer. Glycoconj J 14:569-76.
58. Carvalho AS, Harduin-Lepers A, Magalhães A, Machado E, Mendes N, Costa LT, Matthiesen R, Almeida R, Costa J, Reis CA. 2010. Differential expression of alpha-2,3-sialyltransferases and alpha-1,3/4-fucosyltransferases regulates the levels of sialyl Lewis a and sialyl Lewis x in gastrointestinal carcinoma cells. Int J Biochem Cell Biol 42:80-9.
59. Dennis JW, Laferté S, Waghorne C, Breitman ML, Kerbel RS. 1987. Beta 1-6 branching of Asn-linked oligosaccharides is directly associated with metastasis. Science 236:582-5.
60. Pinho SS, Reis CA. 2015. Glycosylation in cancer: mechanisms and clinical implications. Nat Rev Cancer 15:540-55.
61. Kudelka MR, Ju T, Heimburg-Molinaro J, Cummings RD. 2015. Simple sugars to complex disease--mucin-type O-glycans in cancer. Adv Cancer Res 126:53-135.
62. Helenius A, Aebi M. 2001. Intracellular functions of N-linked glycans. Science 291:2364-9.
63. Pinho SS, Seruca R, Gärtner F, Yamaguchi Y, Gu J, Taniguchi N, Reis CA. 2011. Modulation of E-cadherin function and dysfunction by N-glycosylation. Cell Mol Life Sci 68:1011-20.
64. Paredes J, Figueiredo J, Albergaria A, Oliveira P, Carvalho J, Ribeiro AS, Caldeira J, Costa AM, Simões-Correia J, Oliveira MJ, Pinheiro H, Pinho SS, Mateus R, Reis CA, Leite M, Fernandes MS, Schmitt F, Carneiro F, Figueiredo C, Oliveira C, Seruca R. 2012. Epithelial E- and P-cadherins: role and clinical significance in cancer. Biochim Biophys Acta 1826:297-311.
65. Gu J, Sato Y, Kariya Y, Isaji T, Taniguchi N, Fukuda T. 2009. A mutual regulation between cell-cell adhesion and N-glycosylation: implication of the bisecting GlcNAc for biological functions. J Proteome Res 8:431-5.
66. Dennis JW, Granovsky M, Warren CE. 1999. Glycoprotein glycosylation and cancer progression. Biochim Biophys Acta 1473:21-34.
67. Pinho SS, Reis CA, Gärtner F, Alpaugh ML. 2009. Molecular plasticity of E-cadherin and sialyl lewis x expression, in two comparative models of mammary tumorigenesis. PLoS One 4:e6636.
68. Seidenfaden R, Krauter A, Schertzinger F, Gerardy-Schahn R, Hildebrandt H. 2003. Polysialic acid directs tumor cell growth by controlling heterophilic neural cell adhesion molecule interactions. Mol Cell Biol 23:5908-18.
69. Lin S, Kemmner W, Grigull S, Schlag PM. 2002. Cell surface alpha 2,6 sialylation affects adhesion of breast carcinoma cells. Exp Cell Res 276:101-10.
70. Kim SH, Turnbull J, Guimond S. 2011. Extracellular matrix and cell signalling: the dynamic cooperation of integrin, proteoglycan and growth factor receptor. J Endocrinol 209:139-51.
71. English NM, Lesley JF, Hyman R. 1998. Site-specific de-N-glycosylation of CD44 can activate hyaluronan binding, and CD44 activation states show distinct threshold densities for hyaluronan binding. Cancer Res 58:3736-42.
72. Goupille C, Hallouin F, Meflah K, Le Pendu J. 1997. Increase of rat colon carcinoma cells tumorigenicity by alpha(1-2) fucosyltransferase gene transfection. Glycobiology 7:221-9.

73. Paszek MJ, DuFort CC, Rossier O, Bainer R, Mouw JK, Godula K, Hudak JE, Lakins JN, Wijekoon AC, Cassereau L, Rubashkin MG, Magbanua MJ, Thorn KS, Davidson MW, Rugo HS, Park JW, Hammer DA, Giannone G, Bertozzi CR, Weaver VM. 2014. The cancer glycocalyx mechanically primes integrin-mediated growth and survival. Nature 511:319-25.
74. Tarbell JM, Cancel LM. 2016. The glycocalyx and its significance in human medicine. J Intern Med 280:97-113.
75. Gupta V, Bhinge KN, Hosain SB, Xiong K, Gu X, Shi R, Ho MY, Khoo KH, Li SC, Li YT, Ambudkar SV, Jazwinski SM, Liu YY. 2012. Ceramide glycosylation by glucosylceramide synthase selectively maintains the properties of breast cancer stem cells. J Biol Chem 287:37195-205.
76. Roucourt B, Meeussen S, Bao J, Zimmermann P, David G. 2015. Heparanase activates the syndecan-syntenin-ALIX exosome pathway. Cell Res 25:412-28.
77. Warburg O. 1956. On the origin of cancer cells. Science 123:309-14.
78. Marshall S, Bacote V, Traxinger RR. 1991. Discovery of a metabolic pathway mediating glucose-induced desensitization of the glucose transport system. Role of hexosamine biosynthesis in the induction of insulin resistance. J Biol Chem 266:4706-12.
79. Wells L, Vosseller K, Hart GW. 2001. Glycosylation of nucleocytoplasmic proteins: signal transduction and O-GlcNAc. Science 291:2376-8.
80. Slawson C, Copeland RJ, Hart GW. 2010. O-GlcNAc signaling: a metabolic link between diabetes and cancer? Trends Biochem Sci 35:547-55.
81. Rabinovich GA, Toscano MA. 2009. Turning 'sweet' on immunity: galectin-glycan interactions in immune tolerance and inflammation. Nat Rev Immunol 9:338-52.
82. Macauley MS, Crocker PR, Paulson JC. 2014. Siglec-mediated regulation of immune cell function in disease. Nat Rev Immunol 14:653-66.
83. Ragupathi G, Liu NX, Musselli C, Powell S, Lloyd K, Livingston PO. 2005. Antibodies against tumor cell glycolipids and proteins, but not mucins, mediate complement-dependent cytotoxicity. J Immunol 174:5706-12.
84. Lavrsen K, Madsen CB, Rasch MG, Woetmann A, Ødum N, Mandel U, Clausen H, Pedersen AE, Wandall HH. 2013. Aberrantly glycosylated MUC1 is expressed on the surface of breast cancer cells and a target for antibody-dependent cell-mediated cytotoxicity. Glycoconj J 30:227-36.
85. Saeland E, van Vliet SJ, Bäckström M, van den Berg VC, Geijtenbeek TB, Meijer GA, van Kooyk Y. 2007. The C-type lectin MGL expressed by dendritic cells detects glycan changes on MUC1 in colon carcinoma. Cancer Immunol Immunother 56:1225-36.
86. Samsen A, Bogoevska V, Klampe B, Bamberger AM, Lucka L, Horst AK, Nollau P, Wagener C. 2010. DC-SIGN and SRCL bind glycans of carcinoembryonic antigen (CEA) and CEA-related cell adhesion molecule 1 (CEACAM1): recombinant human glycan-binding receptors as analytical tools. Eur J Cell Biol 89:87-94.
87. Szczykutowicz J. 2023. Ligand Recognition by the Macrophage Galactose-Type C-Type Lectin: Self or Non-Self?-A Way to Trick the Host's Immune System. Int J Mol Sci 24.
88. Im A, Pavletic SZ. 2017. Immunotherapy in hematologic malignancies: past, present, and future. J Hematol Oncol 10:94.
89. Noh J-Y, Seo H, Lee J, Jung H. 2020. Immunotherapy in Hematologic Malignancies: Emerging Therapies and Novel Approaches. International Journal of Molecular Sciences 21:8000.

90. Anonymous. 2017. First-Ever CAR T-cell Therapy Approved in U.S. Cancer Discovery 7:OF1-OF1.
91. Anonymous. 2018. FDA Approves Second CAR T-cell Therapy. Cancer Discov 8:5-6.
92. Mullard A. 2021. FDA approves fourth CAR-T cell therapy. Nat Rev Drug Discov 20:166.
93. Freitag F, Maucher M, Riester Z, Hudecek M. 2020. New targets and technologies for CAR-T cells. Curr Opin Oncol 32:510-517.
94. Hay KA. 2018. Cytokine release syndrome and neurotoxicity after CD19 chimeric antigen receptor-modified (CAR-) T cell therapy. Br J Haematol 183:364-374.
95. Kochenderfer JN, Dudley ME, Feldman SA, Wilson WH, Spaner DE, Maric I, Stetler-Stevenson M, Phan GQ, Hughes MS, Sherry RM, Yang JC, Kammula US, Devillier L, Carpenter R, Nathan DA, Morgan RA, Laurencot C, Rosenberg SA. 2012. B-cell depletion and remissions of malignancy along with cytokine-associated toxicity in a clinical trial of anti-CD19 chimeric-antigen-receptor-transduced T cells. Blood 119:2709-20.
96. Ruella M, Maus MV. 2016. Catch me if you can: Leukemia Escape after CD19-Directed T Cell Immunotherapies. Comput Struct Biotechnol J 14:357-362.
97. Depil S, Duchateau P, Grupp SA, Mufti G, Poirot L. 2020. 'Off-the-shelf' allogeneic CAR T cells: development and challenges. Nat Rev Drug Discov 19:185-199.
98. Chiossone L, Dumas PY, Vienne M, Vivier E. 2018. Natural killer cells and other innate lymphoid cells in cancer. Nat Rev Immunol 18:671-688.
99. Kiessling R, Klein E, Pross H, Wigzell H. 1975. "Natural" killer cells in the mouse. II. Cytotoxic cells with specificity for mouse Moloney leukemia cells. Characteristics of the killer cell. Eur J Immunol 5:117-21.
100. De Maria A, Bozzano F, Cantoni C, Moretta L. 2011. Revisiting human natural killer cell subset function revealed cytolytic CD56(dim)CD16+ NK cells as rapid producers of abundant IFN-gamma on activation. Proc Natl Acad Sci U S A 108:728-32.
101. Passweg JR, Tichelli A, Meyer-Monard S, Heim D, Stern M, Kühne T, Favre G, Gratwohl A. 2004. Purified donor NK-lymphocyte infusion to consolidate engraftment after haploidentical stem cell transplantation. Leukemia 18:1835-8.
102. Olson JA, Leveson-Gower DB, Gill S, Baker J, Beilhack A, Negrin RS. 2010. NK cells mediate reduction of GVHD by inhibiting activated, alloreactive T cells while retaining GVT effects. Blood 115:4293-301.
103. Shaffer BC, Le Luduec JB, Forlenza C, Jakubowski AA, Perales MA, Young JW, Hsu KC. 2016. Phase II Study of Haploidentical Natural Killer Cell Infusion for Treatment of Relapsed or Persistent Myeloid Malignancies Following Allogeneic Hematopoietic Cell Transplantation. Biol Blood Marrow Transplant 22:705-709.
104. Ruggeri L, Capanni M, Urbani E, Perruccio K, Shlomchik WD, Tosti A, Posati S, Rogaia D, Frassoni F, Aversa F, Martelli MF, Velardi A. 2002. Effectiveness of donor natural killer cell alloreactivity in mismatched hematopoietic transplants. Science 295:2097-100.
105. Floros T, Tarhini AA. 2015. Anticancer Cytokines: Biology and Clinical Effects of Interferon-α2, Interleukin (IL)-2, IL-15, IL-21, and IL-12. Semin Oncol 42:539-48.
106. Gauthier M, Laroye C, Bensoussan D, Boura C, Decot V. 2021. Natural Killer cells and monoclonal antibodies: Two partners for successful antibody dependent cytotoxicity against tumor cells. Crit Rev Oncol Hematol 160:103261.
107. Gleason MK, Verneris MR, Todhunter DA, Zhang B, McCullar V, Zhou SX, Panoskaltsis-Mortari A, Weiner LM, Vallera DA, Miller JS. 2012. Bispecific and trispecific killer cell engagers directly activate human NK cells through CD16

signaling and induce cytotoxicity and cytokine production. Mol Cancer Ther 11:2674-84.
108. Ok CY, Young KH. 2017. Checkpoint inhibitors in hematological malignancies. J Hematol Oncol 10:103.
109. Muntasell A, Ochoa MC, Cordeiro L, Berraondo P, López-Díaz de Cerio A, Cabo M, López-Botet M, Melero I. 2017. Targeting NK-cell checkpoints for cancer immunotherapy. Curr Opin Immunol 45:73-81.
110. Korde N, Carlsten M, Lee MJ, Minter A, Tan E, Kwok M, Manasanch E, Bhutani M, Tageja N, Roschewski M, Zingone A, Costello R, Mulquin M, Zuchlinski D, Maric I, Calvo KR, Braylan R, Tembhare P, Yuan C, Stetler-Stevenson M, Trepel J, Childs R, Landgren O. 2014. A phase II trial of pan-KIR2D blockade with IPH2101 in smoldering multiple myeloma. Haematologica 99:e81-3.
111. Ruggeri L, Urbani E, André P, Mancusi A, Tosti A, Topini F, Bléry M, Animobono L, Romagné F, Wagtmann N, Velardi A. 2016. Effects of anti-NKG2A antibody administration on leukemia and normal hematopoietic cells. Haematologica 101:626-33.
112. Caruso S, De Angelis B, Carlomagno S, Del Bufalo F, Sivori S, Locatelli F, Quintarelli C. 2020. NK cells as adoptive cellular therapy for hematological malignancies: Advantages and hurdles. Semin Hematol 57:175-184.
113. Smith SM, Wachter K, Burris HA, 3rd, Schilsky RL, George DJ, Peterson DE, Johnson ML, Markham MJ, Mileham KF, Beg MS, Bendell JC, Dreicer R, Keedy VL, Kimple RJ, Knoll MA, LoConte N, MacKay H, Meisel JL, Moynihan TJ, Mulrooney DA, Mulvey TM, Odenike O, Pennell NA, Reeder-Hayes K, Smith C, Sullivan RJ, Uzzo R. 2021. Clinical Cancer Advances 2021: ASCO's Report on Progress Against Cancer. J Clin Oncol 39:1165-1184.
114. Robert C. 2020. A decade of immune-checkpoint inhibitors in cancer therapy. Nat Commun 11:3801.
115. Ledford H. 2011. Melanoma drug wins US approval. Nature 471:561.
116. Shiravand Y, Khodadadi F, Kashani SMA, Hosseini-Fard SR, Hosseini S, Sadeghirad H, Ladwa R, O'Byrne K, Kulasinghe A. 2022. Immune Checkpoint Inhibitors in Cancer Therapy. Curr Oncol 29:3044-3060.
117. Johnson DB, Nebhan CA, Moslehi JJ, Balko JM. 2022. Immune-checkpoint inhibitors: long-term implications of toxicity. Nat Rev Clin Oncol 19:254-267.
118. Cai X, Zhan H, Ye Y, Yang J, Zhang M, Li J, Zhuang Y. 2021. Current Progress and Future Perspectives of Immune Checkpoint in Cancer and Infectious Diseases. Front Genet 12:785153.
119. Pardoll DM. 2012. The blockade of immune checkpoints in cancer immunotherapy. Nat Rev Cancer 12:252-64.
120. Sadeghi Rad H, Monkman J, Warkiani ME, Ladwa R, O'Byrne K, Rezaei N, Kulasinghe A. 2021. Understanding the tumor microenvironment for effective immunotherapy. Med Res Rev 41:1474-1498.
121. Seidel JA, Otsuka A, Kabashima K. 2018. Anti-PD-1 and Anti-CTLA-4 Therapies in Cancer: Mechanisms of Action, Efficacy, and Limitations. Front Oncol 8:86.
122. Lu H, Zhao X, Li Z, Hu Y, Wang H. 2021. From CAR-T Cells to CAR-NK Cells: A Developing Immunotherapy Method for Hematological Malignancies. Frontiers in Oncology 11.
123. Zhang C, Liu J, Zhong JF, Zhang X. 2017. Engineering CAR-T cells. Biomark Res 5:22.

124. Weinkove R, George P, Dasyam N, McLellan AD. 2019. Selecting costimulatory domains for chimeric antigen receptors: functional and clinical considerations. Clinical & Translational Immunology 8:e1049.
125. Chmielewski M, Abken H. 2015. TRUCKs: the fourth generation of CARs. Expert Opin Biol Ther 15:1145-54.
126. Töpfer K, Cartellieri M, Michen S, Wiedemuth R, Müller N, Lindemann D, Bachmann M, Füssel M, Schackert G, Temme A. 2015. DAP12-based activating chimeric antigen receptor for NK cell tumor immunotherapy. J Immunol 194:3201-12.
127. Billadeau DD, Upshaw JL, Schoon RA, Dick CJ, Leibson PJ. 2003. NKG2D-DAP10 triggers human NK cell-mediated killing via a Syk-independent regulatory pathway. Nat Immunol 4:557-64.
128. Xie G, Dong H, Liang Y, Ham JD, Rizwan R, Chen J. 2020. CAR-NK cells: A promising cellular immunotherapy for cancer. EBioMedicine 59:102975.
129. Imai C, Iwamoto S, Campana D. 2005. Genetic modification of primary natural killer cells overcomes inhibitory signals and induces specific killing of leukemic cells. Blood 106:376-83.
130. Boissel L, Betancur M, Lu W, Wels WS, Marino T, Van Etten RA, Klingemann H. 2012. Comparison of mRNA and lentiviral based transfection of natural killer cells with chimeric antigen receptors recognizing lymphoid antigens. Leuk Lymphoma 53:958-65.
131. Xiao L, Cen D, Gan H, Sun Y, Huang N, Xiong H, Jin Q, Su L, Liu X, Wang K, Yan G, Dong T, Wu S, Zhou P, Zhang J, Liang W, Ren J, Teng Y, Chen C, Xu XH. 2019. Adoptive Transfer of NKG2D CAR mRNA-Engineered Natural Killer Cells in Colorectal Cancer Patients. Mol Ther 27:1114-1125.
132. Oei VYS, Siernicka M, Graczyk-Jarzynka A, Hoel HJ, Yang W, Palacios D, Almåsbak H, Bajor M, Clement D, Brandt L, Önfelt B, Goodridge J, Winiarska M, Zagozdzon R, Olweus J, Kyte JA, Malmberg KJ. 2018. Intrinsic Functional Potential of NK-Cell Subsets Constrains Retargeting Driven by Chimeric Antigen Receptors. Cancer Immunol Res 6:467-480.
133. Schmidt P, Raftery MJ, Pecher G. 2020. Engineering NK Cells for CAR Therapy-Recent Advances in Gene Transfer Methodology. Front Immunol 11:611163.
134. Hudecek M, Ivics Z. 2018. Non-viral therapeutic cell engineering with the Sleeping Beauty transposon system. Curr Opin Genet Dev 52:100-108.
135. Kim A, Pyykko I. 2011. Size matters: versatile use of PiggyBac transposons as a genetic manipulation tool. Mol Cell Biochem 354:301-9.
136. Hu Y, Tian ZG, Zhang C. 2018. Chimeric antigen receptor (CAR)-transduced natural killer cells in tumor immunotherapy. Acta Pharmacol Sin 39:167-176.
137. Chan LY DS, Tye GJ, Imran SAM, Wan Kamarul Zaman WS, Nordin F. 2022. CAR-T Cells/-NK Cells in Cancer Immunotherapy and the Potential of MSC to Enhance Its Efficacy: A Review. Biomedicines 10:804.
138. Klingemann H. 2014. Are natural killer cells superior CAR drivers? Oncoimmunology 3:e28147.
139. Zhang L, Chu J, Yu J, Wei W. 2016. Cellular and molecular mechanisms in graft-versus-host disease. J Leukoc Biol 99:279-87.
140. Ingegnere T, Mariotti FR, Pelosi A, Quintarelli C, De Angelis B, Tumino N, Besi F, Cantoni C, Locatelli F, Vacca P, Moretta L. 2019. Human CAR NK Cells: A New Non-viral Method Allowing High Efficient Transfection and Strong Tumor Cell Killing. Front Immunol 10:957.

141. Yu J, Freud AG, Caligiuri MA. 2013. Location and cellular stages of natural killer cell development. Trends Immunol 34:573-82.
142. Altvater B, Landmeier S, Pscherer S, Temme J, Schweer K, Kailayangiri S, Campana D, Juergens H, Pule M, Rossig C. 2009. 2B4 (CD244) signaling by recombinant antigen-specific chimeric receptors costimulates natural killer cell activation to leukemia and neuroblastoma cells. Clin Cancer Res 15:4857-66.
143. Xu Y, Liu Q, Zhong M, Wang Z, Chen Z, Zhang Y, Xing H, Tian Z, Tang K, Liao X, Rao Q, Wang M, Wang J. 2019. 2B4 costimulatory domain enhancing cytotoxic ability of anti-CD5 chimeric antigen receptor engineered natural killer cells against T cell malignancies. J Hematol Oncol 12:49.
144. Geller MA, Miller JS. 2011. Use of allogeneic NK cells for cancer immunotherapy. Immunotherapy 3:1445-59.
145. Klingemann H. 2015. Challenges of cancer therapy with natural killer cells. Cytotherapy 17:245-9.
146. van Ostaijen-ten Dam MM, Prins HJ, Boerman GH, Vervat C, Pende D, Putter H, Lankester A, van Tol MJ, Zwaginga JJ, Schilham MW. 2016. Preparation of Cytokine-activated NK Cells for Use in Adoptive Cell Therapy in Cancer Patients: Protocol Optimization and Therapeutic Potential. J Immunother 39:90-100.
147. Murray S, Lundqvist A. 2016. Targeting the tumor microenvironment to improve natural killer cell-based immunotherapies: On being in the right place at the right time, with resilience. Hum Vaccin Immunother 12:607-11.
148. Bi J, Tian Z. 2019. NK Cell Dysfunction and Checkpoint Immunotherapy. Front Immunol 10:1999.
149. Konjević GM, Vuletić AM, Mirjačić Martinović KM, Larsen AK, Jurišić VB. 2019. The role of cytokines in the regulation of NK cells in the tumor environment. Cytokine 117:30-40.
150. Domogala A, Madrigal JA, Saudemont A. 2016. Cryopreservation has no effect on function of natural killer cells differentiated in vitro from umbilical cord blood CD34(+) cells. Cytotherapy 18:754-9.
151. Liu E, Marin D, Banerjee P, Macapinlac HA, Thompson P, Basar R, Nassif Kerbauy L, Overman B, Thall P, Kaplan M, Nandivada V, Kaur I, Nunez Cortes A, Cao K, Daher M, Hosing C, Cohen EN, Kebriaei P, Mehta R, Neelapu S, Nieto Y, Wang M, Wierda W, Keating M, Champlin R, Shpall EJ, Rezvani K. 2020. Use of CAR-Transduced Natural Killer Cells in CD19-Positive Lymphoid Tumors. N Engl J Med 382:545-553.
152. Liu E, Tong Y, Dotti G, Shaim H, Savoldo B, Mukherjee M, Orange J, Wan X, Lu X, Reynolds A, Gagea M, Banerjee P, Cai R, Bdaiwi MH, Basar R, Muftuoglu M, Li L, Marin D, Wierda W, Keating M, Champlin R, Shpall E, Rezvani K. 2018. Cord blood NK cells engineered to express IL-15 and a CD19-targeted CAR show long-term persistence and potent antitumor activity. Leukemia 32:520-531.
153. Daher M, Basar R, Gokdemir E, Baran N, Uprety N, Nunez Cortes AK, Mendt M, Kerbauy LN, Banerjee PP, Shanley M, Imahashi N, Li L, Lim F, Fathi M, Rezvan A, Mohanty V, Shen Y, Shaim H, Lu J, Ozcan G, Ensley E, Kaplan M, Nandivada V, Bdiwi M, Acharya S, Xi Y, Wan X, Mak D, Liu E, Jiang XR, Ang S, Muniz-Feliciano L, Li Y, Wang J, Kordasti S, Petrov N, Varadarajan N, Marin D, Brunetti L, Skinner RJ, Lyu S, Silva L, Turk R, Schubert MS, Rettig GR, McNeill MS, Kurgan G, Behlke MA, Li H, Fowlkes NW, et al. 2021. Targeting a cytokine checkpoint enhances the fitness of armored cord blood CAR-NK cells. Blood 137:624-636.
154. Bailey SR, Maus MV. 2019. Gene editing for immune cell therapies. Nat Biotechnol 37:1425-1434.

155. Testa U, Pelosi E, Castelli G. 2019. CD123 as a Therapeutic Target in the Treatment of Hematological Malignancies. Cancers 11:1358.
156. Baumeister SH, Murad J, Werner L, Daley H, Trebeden-Negre H, Gicobi JK, Schmucker A, Reder J, Sentman CL, Gilham DE, Lehmann FF, Galinsky I, DiPietro H, Cummings K, Munshi NC, Stone RM, Neuberg DS, Soiffer R, Dranoff G, Ritz J, Nikiforow S. 2019. Phase I Trial of Autologous CAR T Cells Targeting NKG2D Ligands in Patients with AML/MDS and Multiple Myeloma. Cancer Immunol Res 7:100-112.
157. Daher M, Rezvani K. 2021. Outlook for New CAR-Based Therapies with a Focus on CAR NK Cells: What Lies Beyond CAR-Engineered T Cells in the Race against Cancer. Cancer Discov 11:45-58.
158. Ljunggren HG, Kärre K. 1990. In search of the 'missing self': MHC molecules and NK cell recognition. Immunol Today 11:237-44.
159. ATCC. MCF7. https://www.atcc.org/products/htb-22. Accessed 6 April.
160. ATCC. MDA-MB-231. https://www.atcc.org/products/htb-26#detailed-product-information. Accessed 6 April 2024.
161. ATCC. Het-1A. https://www.atcc.org/products/crl-2692. Accessed 6 April.
162. Cellosaurus. 05-Oct-2024. Cellosaurus Jurkat-TAg (CVCL_C831). https://www.cellosaurus.org/CVCL_C831. Accessed 14. April.
163. Cellosaurus. 30-Jan-2024. Cellosaurus KYSE-450 (CVCL_1353). https://www.cellosaurus.org/CVCL_1353. Accessed 12. April.
164. ATCC. T-47D. https://www.atcc.org/products/htb-133. Accessed 6 April.
165. ATCC. THP-1. https://www.atcc.org/products/tib-202. Accessed 6 April.
166. ATCC. SK-BR-3 [SKBR3]. https://www.atcc.org/products/htb-30. Accessed 6 April.
167. Cellosaurus. 05-Oct-2024. Cellosaurus WM35 (CVCL_0580). https://www.cellosaurus.org/CVCL_0580. Accessed 14. April.
168. Wang D, Kuzyk V, Madunić K, Zhang T, Mayboroda OA, Wuhrer M, Lageveen-Kammeijer GSM. 2023. In-Depth Analysis of the N-Glycome of Colorectal Cancer Cell Lines. International Journal of Molecular Sciences 24:4842.
169. Adan A, Alizada G, Kiraz Y, Baran Y, Nalbant A. 2017. Flow cytometry: basic principles and applications. Crit Rev Biotechnol 37:163-176.
170. Suzuki M, Hayashi H, Mizuki T, Maekawa T, Morimoto H. 2016. Efficient DNA ligation by selective heating of DNA ligase with a radio frequency alternating magnetic field. Biochem Biophys Rep 8:360-364.
171. Lorenz TC. 2012. Polymerase chain reaction: basic protocol plus troubleshooting and optimization strategies. J Vis Exp doi:10.3791/3998:e3998.
172. Anonymous. Benchling. https://www.benchling.com. Accessed
173. Miller AD. 2014. Retroviral vectors: from cancer viruses to therapeutic tools. Hum Gene Ther 25:989-94.
174. Labbé RP, Vessillier S, Rafiq QA. 2021. Lentiviral Vectors for T Cell Engineering: Clinical Applications, Bioprocessing and Future Perspectives. Viruses 13.

# Appendices

## Appendix A – Equipment and instruments

**Table A1 – Equipment.** List of equipment used in this project.

| Equipment | Manufacture |
|---|---|
| Eppendorf tubes | Eppendorf |
| Falcon tubes | Falcon |
| HiClave HV-110 | HMC |
| Nunc™ Petri dishes 90 mm | Thermo Scientific |
| Pipetboy | Integra Bioscience |
| Pipette | Thermo Scientific |
| T175 Nunc™ Non-treated Flasks | Thermo Scientific |
| T225 Nunc™ Non-treated Flasks | Thermo Scientific |
| 96 Conical (V) Bottom Plate, Non-Treated Surface | Thermo Scientific |

**Table A2 – Instruments.** List of instruments used in this project.

| Instrument | Manufacture |
|---|---|
| Centrifuge 5424 | Eppendorf™ |
| Digital Graphic printer UP-D897 | SONY |
| Electrophoresis power supply EPS 301 | Amersham Pharmacia Biotech |
| FACSCalibur™ Flow Cytometer | BD Biosciences |
| GeneAmp machin System 9700 | Applied Biosystems |
| GoTaq G2 Flexi, DNA Polymerase | Promega |
| Imaging system, Benchtop UV, Transilluminator, UVP | BioDoc-It |
| Incubator shaker series | Innova 44 |
| Mini horizontal submarine unit HE33 | Hoefer |
| Nanodrop One | Thermo Scientific |
| Rotina 420R Centrifuge | Hettich |
| TC20 Automated Cell Counder | BioRad |
| T4 DNA Ligase, LC | Thermo Scientific |
| UV-light LKB 2011 | Macrovue Transilluminator |

## Appendix B - Chemicals and reagents

Wendi Jensen produced the fusion proteins used in this project (listed in table 3.2) and Michael Rory Daws produced and isolated the LMI competent DH5α E. coli. dNTP 5mM and BpBlue dye (6 x) was portion out in several Eppendorf tubes, the original packaging of these was therefore untraceable.

**Table B1 – Chemicals and reagents.** List of chemicals and reagents used in this project.

| Chemicals/reagent product name | Cat. No. | Manufacture |
|---|---|---|
| Affini Pure™ Donkey Anti-Human IgG Fcγ fragment specific | | Jackson ImmunoResearch |
| Alkaline phosphatase, Calf intestinal (CIP) | M0290S | New England BioLabs |
| Bam HI | R0136S | New England BioLabs |
| Bgl II | R0144S | New England BioLabs |
| BpBlue dye (6 x) buffer EDTA/BpBlue/XyCy/Glycerol | | |
| CutSmart | B7204S | New England BioLabs |
| DMEM Medium | 11965092 | Gibco |
| dNTP 5mM | | |
| Ethidium bromide | 15585011 | Invitogen™ |
| GoTaq G2 Flexi DNA Polymerase | M780B | Promega |
| LMI competent DH5α E. coli | | |
| $MgCl_2$ 25 mM | A351H | Promega |
| $MgSO_4$ Stock Solution | 1067200 | Roche Diagnostics |
| NEBuffer 3.1 (10 x) | B7203S | New England BioLabs |
| Nuclease Free Water | P119A | Promega |
| SOC Medium | 15544034 | Invitogen™ |
| TopVision Agarose | R0491 | Thermo Scientific™ |
| UltraPure™ LMP Agarose | 16520050 | Invitogen™ |
| 1 kB DNA Ladder | SM0311 | GeneRuler |
| 5 x Green GoTaq Flexi Buffer | M891A | Promega |
| 10 x Buffer for T4 DNA Ligase ATP | B0202S | New England BioLabs |
| 100 bp Plus | SM0321 | GeneRuler |

**Table B2 – Kits.**

| Kit | Cat. No. | Manufacture |
|---|---|---|
| PCR & Gel Clean up kit (100) | 28506 | QIAGEN |
| QIAprep Spin Miniprep Kit (250) | 27106 | QIAGEN |

**Table B3 – Solutions composition.** Composition of solutions used in this project. Note different total volume for each solutions as well as different units under quantity for each solution.

| Total volume | Solution | Substance | Quantity |
|---|---|---|---|
| 200 mL | **LMP Agarose gel 1,5 %** | UltraPure™ LMP Agarose | 1,5 % |
| | | 1x TAE | 200 mL |
| 200 mL | **Agarose gel 1,5 %** | TopVision Agarose | 1,5 % |
| | | 1x TAE | 200 mL |
| 500 mL | **EMDM (1x) Medium with** | Antibiotic | 0,01 % |
| | | Serum | 10,00 % |
| | | Pyruvate | 0,01 % |
| 500 mL | **100x FACS Additive II** | Azide | 25,00 % |
| | | BSA | 5,00% |
| | | $CaCl_2$ (1M) | 250 µL |
| | | $MgCl_2$ (1M) | 400 µL |
| | | PBS | 500 mL |
| 50 mL | **PBS-EDTA** | PBS | 50 mL |
| | | EDTA 1 mM | 0,1 mL |
| | | FCS | 0,25 mL |
| 50 mL | **PFA with PBS** | $ddH_2O$ | 40 mL |
| | | PFA | 2 g |
| | | PBS (10x) | 5 mL |
| 200 mL | **50x TAE** | $ddH_2O$ | 200 mL |
| | | Tris base | 48,4 g |
| | | Acetic acid | 11,4 mL |
| | | EDTA (0,5 M, pH 8,0) | 20 mL |

## Appendix C – Software and websites

**Table C1 – Software and websites**. List of software and websites used during this project.

| Software/websites | Reference |
|---|---|
| Benchling | https://www.benchling.com |
| BioRender | https://www.biorender.com |
| FlowJo | https://www.flowjo.com/solutions/flowjo |
| GraphPad | https://www.graphpad.com |

## Appendix D – Raw data FACS

Raw data exported from Excel, from FACS runs that were used to make graphs in GraphPad.

### Table D1 – Raw data SKBR3.

| | SKBR3 02.02 | SKBR3 21.03 | SKBR3 02.02 | SKBR3 21.03 |
|---|---|---|---|---|
| **Without FP** | 9,03 | 18,7 | 1 | 1 |
| **CLEC 4D** | 12,7 | 33 | 1,406423034 | 1,764705882 |
| **CLEC 4E** | 10,8 | 31,5 | 1,196013289 | 1,684491979 |
| **CLEC 12A** | 12,3 | 47,4 | 1,362126246 | 2,534759358 |
| **CLEC 1B** | 17 | 36,4 | 1,882613511 | 1,946524064 |
| **CLEC 2D** | 144 | 34,8 | 15,94684385 | 1,860962567 |
| **CLEC 4L** | 9,06 | 1576 | 1,003322259 | 84,27807487 |
| **CLEC 7A** | 8,49 | 25,3 | 0,940199336 | 1,352941176 |
| **CLEC 2A** | 11,3 | 21,4 | 1,251384275 | 1,144385027 |
| **CLEC 8A** | 32,8 | 49,5 | 3,632336656 | 2,647058824 |
| **CLEC 3B** | 9,92 | 64,7 | 1,098560354 | 3,459893048 |
| **CLEC 5A** | 11,6 | 17,4 | 1,284606866 | 0,930481283 |
| **CLEC 1A** | 25,2 | 18,8 | 2,790697674 | 1,005347594 |
| **CLEC 9A** | 8,93 | 84,2 | 0,988925803 | 4,502673797 |
| **CLEC 12B** | | 32,6 | 0 | 1,743315508 |

### Table D2 – Raw data HET-1A.

| | HET 1A 02.02 | HET 1A 21.03 | HET 1A 02.02 | HET 1A 21.03 |
|---|---|---|---|---|
| **Without FP** | 14,1 | 8,95 | 1 | 1 |
| **CLEC 4D** | 19,5 | 18,4 | 1,382978723 | 2,055865922 |
| **CLEC 4E** | 21,9 | 15 | 1,553191489 | 1,675977654 |
| **CLEC 12A** | 15,8 | 15,8 | 1,120567376 | 1,765363128 |
| **CLEC 1B** | 76,3 | 78,9 | 5,411347518 | 8,815642458 |
| **CLEC 2D** | 72,6 | 14,8 | 5,14893617 | 1,653631285 |
| **CLEC 4L** | 13,5 | 67,5 | 0,957446809 | 7,541899441 |
| **CLEC 7A** | 14,3 | 17,9 | 1,014184397 | 2 |
| **CLEC 2A** | 21,2 | 10,7 | 1,503546099 | 1,195530726 |
| **CLEC 8A** | 22,9 | 20,6 | 1,624113475 | 2,301675978 |
| **CLEC 3B** | 16,2 | 25,5 | 1,14893617 | 2,849162011 |
| **CLEC 5A** | 28,7 | 10,1 | 2,035460993 | 1,12849162 |
| **CLEC 1A** | 50,9 | 12 | 3,609929078 | 1,340782123 |
| **CLEC 9A** | 48,8 | 23,2 | 3,460992908 | 2,592178771 |
| **CLEC 12B** | | 42,8 | 0 | 4,782122905 |

**Table D3 – Raw data MDA-MB-231.**

| | MDA-MB-231 02.02 | MDA-MB-231 21.03 | MDA-MB-231 02.02 | MDA-MB-231 21.03 |
|---|---|---|---|---|
| **Without FP** | 6,65 | 7,17 | 1 | 1 |
| **CLEC 4D** | 14 | 9,6 | 2,105263158 | 1,338912134 |
| **CLEC 4E** | 8,17 | 8,6 | 1,228571429 | 1,19944212 |
| **CLEC 12A** | 7,36 | 7,04 | 1,106766917 | 0,981868898 |
| **CLEC 1B** | 8,24 | 10,4 | 1,239097744 | 1,450488145 |
| **CLEC 2D** | 47,9 | 5,49 | 7,203007519 | 0,765690377 |
| **CLEC 4L** | 7,61 | 17,1 | 1,144360902 | 2,384937238 |
| **CLEC 7A** | 7,39 | 7,19 | 1,111278195 | 1,0027894 |
| **CLEC 2A** | 12 | 7,5 | 1,804511278 | 1,046025105 |
| **CLEC 8A** | 16,2 | 10,7 | 2,436090226 | 1,492329149 |
| **CLEC 3B** | 6,55 | 10,1 | 0,984962406 | 1,408647141 |
| **CLEC 5A** | 7,17 | 6,56 | 1,078195489 | 0,914923291 |
| **CLEC 1A** | 17,8 | 7,51 | 2,676691729 | 1,047419805 |
| **CLEC 9A** | 7,53 | 13,8 | 1,132330827 | 1,924686192 |
| **CLEC 12B** | | 9,51 | 0 | 1,326359833 |

**Table D4 – Raw data Jurkat-TAg.**

| | Jurkat-TAg 08.03 | Jurkat-Tag 21.03 | Jurkat-TAg 08.03 | Jurkat-TAg 21.03 |
|---|---|---|---|---|
| **Without FP** | 9,26 | 14,5 | 1 | 1 |
| **CLEC 4D** | 10,9 | 17,9 | 1,177105832 | 1,234482759 |
| **CLEC 4E** | 10,5 | 14,8 | 1,133909287 | 1,020689655 |
| **CLEC 12A** | 7,37 | 15,2 | 0,795896328 | 1,048275862 |
| **CLEC 1B** | 9,2 | 19,1 | 0,993520518 | 1,317241379 |
| **CLEC 2D** | 11,3 | 19,8 | 1,220302376 | 1,365517241 |
| **CLEC 4L** | 30,6 | 27,1 | 3,304535637 | 1,868965517 |
| **CLEC 7A** | 11,1 | 16 | 1,198704104 | 1,103448276 |
| **CLEC 2A** | 9,89 | 15,7 | 1,068034557 | 1,082758621 |
| **CLEC 8A** | 13,9 | 23,4 | 1,501079914 | 1,613793103 |
| **CLEC 3B** | 8,41 | 27,2 | 0,908207343 | 1,875862069 |
| **CLEC 5A** | 10,8 | 14,6 | 1,166306695 | 1,006896552 |
| **CLEC 1A** | 10,2 | 15 | 1,101511879 | 1,034482759 |
| **CLEC 9A** | 15,1 | 20,5 | 1,630669546 | 1,413793103 |
| **CLEC 12B** | 11,3 | 15,4 | 1,220302376 | 1,062068966 |

**Table D5 – Raw data KYSE-450.**

| | KYSE450 02.02 | KYSE450 21.03 | KYSE450 02.02 | KYSE450 21.03 |
|---|---|---|---|---|
| **Without FP** | 8,05 | 17,6 | 1 | 1 |
| **CLEC 4D** | 30,1 | 42,8 | 3,739130435 | 2,431818182 |
| **CLEC 4E** | 15,8 | 22,5 | 1,962732919 | 1,278409091 |
| **CLEC 12A** | 12,6 | 19,6 | 1,565217391 | 1,113636364 |
| **CLEC 1B** | 13,2 | 26,7 | 1,639751553 | 1,517045455 |
| **CLEC 2D** | 129 | 31,4 | 16,02484472 | 1,784090909 |
| **CLEC 4L** | 10,5 | 64,7 | 1,304347826 | 3,676136364 |
| **CLEC 7A** | 8,87 | 17,8 | 1,101863354 | 1,011363636 |
| **CLEC 2A** | 44,6 | 18,6 | 5,540372671 | 1,056818182 |
| **CLEC 8A** | 54,8 | 132 | 6,807453416 | 7,5 |
| **CLEC 3B** | 9,97 | 54,6 | 1,238509317 | 3,102272727 |
| **CLEC 5A** | 14 | 20,6 | 1,739130435 | 1,170454545 |
| **CLEC 1A** | 45,9 | 33 | 5,701863354 | 1,875 |
| **CLEC 9A** | 10,7 | 73,5 | 1,329192547 | 4,176136364 |
| **CLEC 12B** | | 32,4 | 0 | 1,840909091 |

**Table D6 – Raw data T47D, WM35, THP-1**

| | T47D 08.03 | WM25 08.03 | THP-1 08.03 | T47D 08.03 | WM25 08.03 | THP-1 08.03 |
|---|---|---|---|---|---|---|
| **Without FP** | 3,3 | 14,6 | 5,05 | 1 | 1 | 1 |
| **CLEC 4D** | 4,55 | 22,8 | 6 | 1,378787879 | 1,561643836 | 1,188118812 |
| **CLEC 4E** | 3,41 | 17 | 5,52 | 1,033333333 | 1,164383562 | 1,093069307 |
| **CLEC 12A** | 3,26 | 16,2 | 5,29 | 0,987878788 | 1,109589041 | 1,047524752 |
| **CLEC 1B** | 4,45 | 30,7 | 5,75 | 1,348484848 | 2,102739726 | 1,138613861 |
| **CLEC 2D** | 7,52 | 19,9 | 5,47 | 2,278787879 | 1,363013699 | 1,083168317 |
| **CLEC 4L** | 19,7 | 61,1 | 19,9 | 5,96969697 | 4,184931507 | 3,940594059 |
| **CLEC 7A** | 3,79 | 18,1 | 5,11 | 1,148484848 | 1,239726027 | 1,011881188 |
| **CLEC 2A** | 2,37 | 14,7 | 5,3 | 0,718181818 | 1,006849315 | 1,04950495 |
| **CLEC 8A** | 4,58 | 27 | 5,54 | 1,387878788 | 1,849315068 | 1,097029703 |
| **CLEC 3B** | 13,5 | 33,2 | 5,65 | 4,090909091 | 2,273972603 | 1,118811881 |
| **CLEC 5A** | 2,38 | 14,5 | 5,35 | 0,721212121 | 0,993150685 | 1,059405941 |
| **CLEC 1A** | 4,14 | 17,5 | 5,36 | 1,254545455 | 1,198630137 | 1,061386139 |
| **CLEC 9A** | 6,14 | 29,2 | 5,5 | 1,860606061 | 2 | 1,089108911 |
| **CLEC 12B** | 4,13 | 19,8 | 5,29 | 1,251515152 | 1,356164384 | 1,047524752 |

**Table D7 – Raw data MCF7.**

| | MCF7 02.02 | MCF7 13.02 | MCF7 21.03 | MCF7 02.02 | MCF7 13.02 | MCF7 21.03 |
|---|---|---|---|---|---|---|
| **Without FP** | 10,6 | 9,54 | 30,6 | 1 | 1 | 1 |
| **CLEC 4D** | 10,2 | 9,71 | 64,3 | 0,962264151 | 1,01781971 | 2,10130719 |
| **CLEC 4E** | 9,84 | 9,33 | 34,6 | 0,928301887 | 0,97798742 | 1,13071895 |
| **CLEC 12A** | 9,32 | 9,6 | 34,5 | 0,879245283 | 1,00628931 | 1,12745098 |
| **CLEC 1B** | 8,85 | 10,8 | 37,9 | 0,83490566 | 1,13207547 | 1,23856209 |
| **CLEC 2D** | 71,8 | 9,35 | 59,3 | 6,773584906 | 0,98008386 | 1,9379085 |
| **CLEC 4L** | 9,79 | 51,5 | 854 | 0,923584906 | 5,39832285 | 27,9084967 |
| **CLEC 7A** | 8,29 | 9,35 | 80,2 | 0,782075472 | 0,98008386 | 2,62091503 |
| **CLEC 2A** | 10,1 | 8,9 | 30,4 | 0,952830189 | 0,93291405 | 0,99346405 |
| **CLEC 8A** | 10,5 | 10,2 | 81,4 | 0,990566038 | 1,06918239 | 2,66013072 |
| **CLEC 3B** | 8,85 | 10,4 | 103 | 0,83490566 | 1,09014675 | 3,36601307 |
| **CLEC 5A** | 8,64 | 9,87 | 32,1 | 0,81509434 | 1,03459119 | 1,04901961 |
| **CLEC 1A** | 11,9 | 9,6 | 45,2 | 1,122641509 | 1,00628931 | 1,47712418 |
| **CLEC 9A** | 8,07 | 11,3 | 293 | 0,761320755 | 1,18448637 | 9,5751634 |
| **CLEC 12B** | | 10 | 56,7 | 0 | 1,04821803 | 1,85294118 |

**Table D8 – Raw data SF126.**

| | SF126 02.02 | SF126 13.02 | SF126 08.03 | SF126 21.03 | SF126 02.02 | SF126 13.02 | SF126 08.03 | SF126 21.03 |
|---|---|---|---|---|---|---|---|---|
| **Without FP** | 4,64 | 4,06 | 3,37 | 10,6 | 1 | 1 | 1 | 1 |
| **CLEC 4D** | 5,16 | 4,61 | 4,82 | 11,4 | 1,112068966 | 1,13546798 | 1,430267062 | 1,075471698 |
| **CLEC 4E** | 5,01 | 4,25 | 4 | 10,4 | 1,079741379 | 1,04679803 | 1,18694362 | 0,981132075 |
| **CLEC 12A** | 4,82 | 4,2 | 4,33 | 10,3 | 1,038793103 | 1,034482759 | 1,284866469 | 0,971698113 |
| **CLEC 1B** | 4,92 | 4,83 | 5,62 | 9,75 | 1,060344828 | 1,189655172 | 1,667655786 | 0,919811321 |
| **CLEC 2D** | 6,7 | 4,65 | 4,6 | 11 | 1,443965517 | 1,145320197 | 1,364985163 | 1,037735849 |
| **CLEC 4L** | 4,79 | 10,9 | 6,79 | 20,2 | 1,032327586 | 2,684729064 | 2,014836795 | 1,905660377 |
| **CLEC 7A** | 4,63 | 4,29 | 3,9 | 10,5 | 0,997844828 | 1,056650246 | 1,15727003 | 0,990566038 |
| **CLEC 2A** | 5,34 | 4,25 | 3,61 | 10,6 | 1,150862069 | 1,04679803 | 1,071216617 | 1 |
| **CLEC 8A** | 5,08 | 4,85 | 3,94 | 12,6 | 1,094827586 | 1,194581281 | 1,169139466 | 1,188679245 |
| **CLEC 3B** | 4,71 | 5,36 | 4,73 | 11,7 | 1,015086207 | 1,320197044 | 1,403560831 | 1,103773585 |
| **CLEC 5A** | 4,91 | 4,26 | 3,71 | 9,67 | 1,058189655 | 1,049261084 | 1,100890208 | 0,912264151 |
| **CLEC 1A** | 7,24 | 4,46 | 4,11 | 10,3 | 1,560344828 | 1,098522167 | 1,21958457 | 0,971698113 |
| **CLEC 9A** | 4,99 | 11 | 8,13 | 14,2 | 1,075431034 | 2,709359606 | 2,412462908 | 1,339622642 |
| **CLEC 12B** | | 4,26 | 4,13 | 14,7 | 0 | 1,049261084 | 1,225519288 | 1,386792453 |


**Norges miljø- og biovitenskapelige universitet**
Noregs miljø- og biovitskapelege universitet
Norwegian University of Life Sciences

Postboks 5003
NO-1432 Ås
Norway